



In situ isotopic studies of the U-depleted Allende CAI *Curious Marie*: Pre-accretionary alteration and the co-existence of ^{26}Al and ^{36}Cl in the early solar nebula

Haolan Tang^{a,*}, Ming-Chang Liu^a, Kevin D. McKeegan^a, Francois L.H. Tissot^{b,c},
Nicolas Dauphas^b

^a Department of Earth, Planetary, and Space Sciences, UCLA, Los Angeles, CA 90095, United States

^b Origins Lab, Department of the Geophysical Sciences and Enrico Fermi Institute, The University of Chicago, United States

^c Department of the Earth, Atmospheric and Planetary Sciences, MIT, Cambridge 02139, United States

Received 18 August 2016; accepted in revised form 1 March 2017; Available online 18 March 2017

Abstract

The isotopic composition of oxygen as well as ^{26}Al - ^{26}Mg and ^{36}Cl - ^{36}S systematics were studied in *Curious Marie*, an aqueously altered Allende CAI characterized by a Group II REE pattern and a large ^{235}U excess produced by the decay of short-lived ^{247}Cm . Oxygen isotopic compositions in the secondary minerals of *Curious Marie* follow a mass-dependent fractionation line with a relatively homogenous depletion in ^{16}O ($\Delta^{17}\text{O}$ of -8‰) compared to unaltered minerals of CAI components. Both Mg and S show large excesses of radiogenic isotopes ($^{26}\text{Mg}^*$ and $^{36}\text{S}^*$) that are uniformly distributed within the CAI, independent of parent/daughter ratio. A model initial $^{26}\text{Al}/^{27}\text{Al}$ ratio [$(6.2 \pm 0.9) \times 10^{-5}$], calculated using the bulk Al/Mg ratio and the uniform $\delta^{26}\text{Mg}^* \sim +43\text{‰}$, is similar to the canonical initial solar system value within error. The exceptionally high bulk Al/Mg ratio of this CAI (~ 95) compared to other inclusions is presumably due to Mg mobilization by fluids. Therefore, the model initial $^{26}\text{Al}/^{27}\text{Al}$ ratio of this CAI implies not only the early condensation of the CAI precursor but also that aqueous alteration occurred early, when ^{26}Al was still at or near the canonical value. This alteration event is most likely responsible for the U depletion in *Curious Marie* and occurred at most 50 kyr after CAI formation, leading to a revised estimate of the early solar system $^{247}\text{Cm}/^{235}\text{U}$ ratio of $(5.6 \pm 0.3) \times 10^{-5}$. The Mg isotopic composition in *Curious Marie* was subsequently homogenized by closed-system thermal processing without contamination by chondritic Mg. The large, homogeneous ^{36}S excesses ($\Delta^{36}\text{S}^* \sim +97\text{‰}$) detected in the secondary phases of *Curious Marie* are attributed to ^{36}Cl decay ($t_{1/2} = 0.3$ Myr) that was introduced by Cl-rich fluids during the aqueous alteration event that led to sodalite formation. A model $^{36}\text{Cl}/^{35}\text{Cl}$ ratio of $(2.3 \pm 0.6) \times 10^{-5}$ is calculated at the time of aqueous alteration, translating into an initial $^{36}\text{Cl}/^{35}\text{Cl}$ ratio of $\sim 1.7\text{--}3 \times 10^{-5}$ at solar system birth. The Mg and S radiogenic excesses suggest that ^{26}Al and ^{36}Cl co-existed in the early solar nebula, raising the possibility that, in addition to an irradiation origin, ^{36}Cl could have also been derived from a stellar source.

© 2017 Elsevier Ltd. All rights reserved.

Keywords: *Curious Marie* CAI; ^{26}Al - ^{26}Mg systematics; ^{36}Cl - ^{36}S systematics; Aqueous alteration; Origin

1. INTRODUCTION

Extinct radionuclides have proven to be some of the most useful tools for understanding the astrophysical settings of solar system formation, the timescales of events in the early solar system (ESS), the irradiation history of

* Corresponding author.

E-mail address: haolantang@ucla.edu (H. Tang).

early formed solids, and the thermal history of planetary bodies (see reviews by Meyer and Clayton, 2000; McKeegan and Davis, 2004; Wadhwa et al., 2006; Wasserburg et al., 2006; Dauphas and Chaussidon, 2011). Yet, the origin of some of the extinct radionuclides remains a matter of debate. Many of the longer-lived extinct nuclides, such as ^{182}Hf , ^{129}I , and ^{244}Pu , likely originated from the long-term chemical evolution of the Galaxy (Clayton, 1985, 1988; Nittler and Dauphas, 2006; Huss et al., 2009; Young, 2014). On the other hand, some very short-lived radionuclides ($t_{1/2} \leq 1$ Myr), such as ^{26}Al , may come from the stellar winds of one or more nearby massive stars and have been injected either into the molecular cloud from which the Sun formed, or directly into the early solar nebula (Arnould et al., 1997, 2006; Gaidos et al., 2009; Tatischeff et al., 2010; Gounelle and Meynet, 2012; Tang and Dauphas 2012; Jura et al., 2013; Young, 2014; Gounelle, 2015). In such external seeding scenarios, these injected radionuclides can potentially be used as high-resolution chronometers to constrain the evolution of the ESS. In contrast, the presence of other short-lived nuclides in the ESS is best understood as resulting from local irradiation of nebular materials by the proto-Sun (e.g., ^{10}Be , ^{41}Ca , and ^{36}Cl , McKeegan et al., 2000; Marhas et al., 2002; Hsu et al., 2006; Chaussidon and Gounelle, 2006; Duprat and Tatischeff, 2007; Jacobsen et al., 2011; Liu et al., 2012; Bricker and Caffee, 2013; Turner et al., 2013; Trappitsch and Ciesla, 2015). Accordingly, the difference in the abundance of an irradiation-produced short-lived nuclide among various ESS objects does not hold any chronometric information, reflecting instead the irradiation history by particles emanating from the young Sun.

Chlorine-36 ($t_{1/2} = 0.3$ Myr) decays to either ^{36}Ar (98.1%, β^-) or ^{36}S (1.9%, ϵ and β^+). This radionuclide can be produced by irradiation of gas and/or dust of solar composition (Leya et al., 2003; Gounelle et al., 2006). Alternatively, stellar nucleosynthesis in AGB stars or Type II supernovae could account for the presence of ^{36}Cl in the ESS (Wasserburg et al., 2006). Evidence for the prior existence of ^{36}Cl in the ESS comes from radiogenic excesses of ^{36}Ar (Murty et al., 1997; Turner et al., 2013) and/or ^{36}S (Lin et al., 2005; Hsu et al., 2006; Ushikubo et al., 2007; Jacobsen et al., 2011) in secondary phases (e.g., sodalite and wadalite) produced by alteration of Calcium, Aluminum-rich inclusions (CAIs) and chondrules. Though the presence of ^{36}Cl in the ESS has been demonstrated, the inferred initial $^{36}\text{Cl}/^{35}\text{Cl}$ ratios in previous studies vary over two orders of magnitude.

The former presence of ^{36}Cl in the ESS was first detected as radiogenic excesses of ^{36}S in a fine-grained CAI from the Ningqiang chondrite with a CAMECA small geometry ion microprobe (ims-6f). Sodalite-rich alteration assemblages showed clear excesses of ^{36}S that positively correlated with Cl/S ratios, giving a $^{36}\text{Cl}/^{35}\text{Cl}$ ratio at sample formation of 5×10^{-6} (Lin et al., 2005). Similar $^{36}\text{Cl}/^{35}\text{Cl}$ ratios were reported in sodalite from Allende CAIs and a porphyritic olivine chondrule (Hsu et al., 2006; Ushikubo et al., 2007). However, measurements of another suite of CAIs with a Cameca NanoSIMS 50 ion probe failed to reveal clear ^{36}S excesses in sodalite, indicating either heterogeneity

in $^{36}\text{Cl}/^{35}\text{Cl}$ in individual objects or a potential artifact in the sulfur isotopic measurements (Nakashima et al., 2008). Analyses by Jacobsen et al. (2011) revealed significant ^{36}S excesses in wadalite in a coarse-grained igneous Allende CAI, from which a $^{36}\text{Cl}/^{35}\text{Cl}$ ratio of $\sim 2 \times 10^{-5}$ was inferred. Meanwhile, large, yet variable excesses of ^{36}S were observed in a unique Na, Cl, Ca, and Al-rich Allende chondrule *A13509* (Wasserburg et al., 2011). The absence of correlation between ^{36}S excesses and $^{35}\text{Cl}/^{34}\text{S}$ ratios in this object was attributed to local redistribution of radiogenic $^{36}\text{S}^*$ after ^{36}Cl had decayed.

Interestingly, although the initial $^{36}\text{Cl}/^{35}\text{Cl}$ ratios inferred in previous studies vary widely, all secondary phases measured so far lack resolvable ^{26}Mg excesses that could be due to the decay of ^{26}Al ($t_{1/2} = 0.7$ Myr), implying that ^{36}Cl and ^{26}Al may have been produced by different processes and/or incorporated into early Solar System solids at different times. Given that ^{26}Al likely comes from a stellar source (e.g., Villeneuve et al., 2009) and that secondary phases may have formed late, the lack of ^{26}Mg excesses in secondary phases presenting ^{36}S anomalies points to either a very high $^{36}\text{Cl}/^{35}\text{Cl}$ initial ratio ($\sim 10^{-2}$) in the ESS, or a late (>3 Myr after CAI formation) irradiation scenario for the local production of ^{36}Cl (Jacobsen et al., 2011). An inferred initial ratio of $^{36}\text{Cl}/^{35}\text{Cl} \sim 10^{-2}$ far exceeds the predictions from any model of stellar nucleosynthesis; therefore, a late irradiation scenario producing ^{36}Cl at the observed level has been the favored idea. In this framework, ^{36}Cl was produced in the early solar nebula and then incorporated into the CAIs via aqueous alteration, which formed Cl-rich phases, such as sodalite and wadalite.

The Allende fine-grained inclusion *Curious Marie* is a unique CAI, highly depleted in uranium, in which an extremely large ^{235}U excess ($\delta^{235}\text{U} \sim +59\%$ relative to the uranium isotopic standard CRM-112a) was recently identified (Tissot et al., 2016). This provided definitive evidence that ^{247}Cm was alive in the ESS, as previously suggested by Brennecka et al. (2010). *Curious Marie* consists primarily of secondary mineral phases such as sodalite, nepheline, and grossular, and is therefore characterized by a distinctive Mg-poor and Cl-rich bulk chemical composition when compared with common fine-grained CAIs. The Cl-rich phases in this sample are characterized by elevated $^{35}\text{Cl}/^{34}\text{S}$ ratios and therefore provide an excellent opportunity to study Cl-S systematics. In this study, we performed *in situ* isotopic measurements of ^{26}Al - ^{26}Mg , ^{36}Cl - ^{36}S and oxygen isotopic compositions of the *Curious Marie* CAI to better understand the origin and evolution of this unusual sample. Our results constrain the timing of alteration in this sample, as well as the relationship between ^{26}Al and ^{36}Cl in the early solar system.

2. METHOD

2.1. Sample description

Curious Marie is a fine-grained CAI, ~ 1.25 cm long and 0.75 cm wide, that was supplied by the Robert A. Pritzker Center for Meteoritics and Polar Studies at the Field Museum (Chicago). A small chip of the CAI was sampled

by using clean stainless steel tweezers, and mounted in epoxy (Buehler) at the Origins Lab at the University of Chicago. This sample consists of widely-distributed powdery, porous aggregates of sodalite [$\text{Na}_8(\text{Al}_6\text{Si}_6\text{O}_{24})\text{Cl}_2$], nepheline [$(\text{Na}_3\text{K})\text{Al}_4\text{Si}_4\text{O}_{16}$], grossular ($\text{Ca}_3\text{Al}_2\text{Si}_3\text{O}_{12}$), and melilite $((\text{Ca},\text{Na})_2(\text{Al},\text{Mg},\text{Fe}^{2+})[(\text{Al},\text{Si})\text{SiO}_7])$ (Fig. 1), suggesting that this inclusion has been heavily altered from its primary mineralogy. Typically distributed in the peripheral portions of Allende CAIs (Krot et al., 2010; Brearley and Krot, 2013 and references within), sodalite occurs widely throughout the *Curious Marie* CAI. The fine-grained sodalite and nepheline minerals, with interspersed regions of melilite and grossular, are indicative of pervasive aqueous alteration involving Na-Cl-bearing fluids (Kimura and Ikeda, 1995). Bulk measurements carried out by Inductively Coupled Plasma Mass Spectrometry (ICP-MS) show that *Curious Marie* CAI is characterized by a Group II rare earth element (REE) pattern (Tissot et al., 2016), indicating a condensation origin of its precursor minerals (Boynton, 1975; Davis and Grossman, 1979). The high chlorine (~7 wt%), high aluminum (~17 wt%), and low sulfur contents (<0.01 wt%) of sodalite make it an ideal mineral for studying the ^{26}Al - ^{26}Mg and ^{36}Cl - ^{36}S systems.

2.2. Analytical methods

Petrologic and mineralogical studies were carried out using a petrographic microscope and a Tescan scanning electron microscope (SEM) equipped with an energy dispersive spectrometer (EDS) at UCLA. Following the SEM characterization, Mg isotopic compositions were analyzed with the UCLA Cameca IMS-1270, and measurements of oxygen and sulfur isotope compositions were performed on the Cameca IMS-1290 ion microprobe at UCLA.

Magnesium isotopes were measured with a ~15 μm , 2 nA O^- primary ion beam in order to generate sufficient signal. Because of the high Al/Mg ratios of the *Curious Marie* CAI (and that of a Madagascar hibonite standard used for normalization), the signals of Mg isotopes and ^{27}Al were measured with the axial electron multiplier (EM) and an axial Faraday cup, respectively, through a peak jumping mass sequence of 23.5 (to condition the magnet hysteresis), ^{24}Mg , ^{25}Mg , ^{26}Mg and ^{27}Al . The mass-resolving power was set to ~4000 to separate all molecular interferences (e.g., $^{24}\text{MgH}^+$) and doubly charged $^{48}\text{Ca}^{++}$ and $^{48}\text{Ti}^{++}$ from the peaks of interest. Mg isotopic values ($\delta^i\text{Mg}$) are calculated as $\delta^i\text{Mg} = \left(\frac{(^i\text{Mg}/^{24}\text{Mg})_{\text{sample}}}{(^i\text{Mg}/^{24}\text{Mg})_{\text{standard}}} - 1 \right) \times 1000$, where the standard $^{26}\text{Mg}/^{24}\text{Mg}$ ratio is 0.13932 (Catanzaro et al., 1966). A relative sensitivity factor, defined as $A \equiv (^{27}\text{Al}/^{24}\text{Mg})_{\text{true}} / (^{27}\text{Al}^+ / ^{24}\text{Mg}^+)_{\text{measured}}$ was determined to be 1.39 ± 0.04 based on the Madagascar hibonite ($^{27}\text{Al}/^{24}\text{Mg} = 42.7 \pm 0.7$; measured by UCLA JEOL JXA-8200 electron microprobe) and was applied for analyses of all phases in the *Curious Marie* CAI. Nepheline and sodalite are fine-grained, therefore some spots are a mixture of the two phases. The radiogenic excesses of ^{26}Mg were calculated by using an exponential law (Davis et al., 2015) with a fixed $^{25}\text{Mg}/^{24}\text{Mg}$ ratio of 0.12663 and $\beta = 0.5160$ determined from a suite of terrestrial materials (San Carlos olivine, San Carlos pyroxene, synthetic pyroxene glass, and Burma spinel, Fig. 2).

Oxygen isotopic measurements were performed at high mass resolution with a beam spot size of ~10 μm . The analytical procedure generally followed the method described in McKeegan et al. (1998). Care was taken to polish the sample mount in order to eliminate the implanted ^{16}O from the primary O^- beam used during Al-Mg *in situ* analysis. A focused Cs^+ primary beam with an intensity of 7 nA was utilized and a normal incidence electron gun was applied

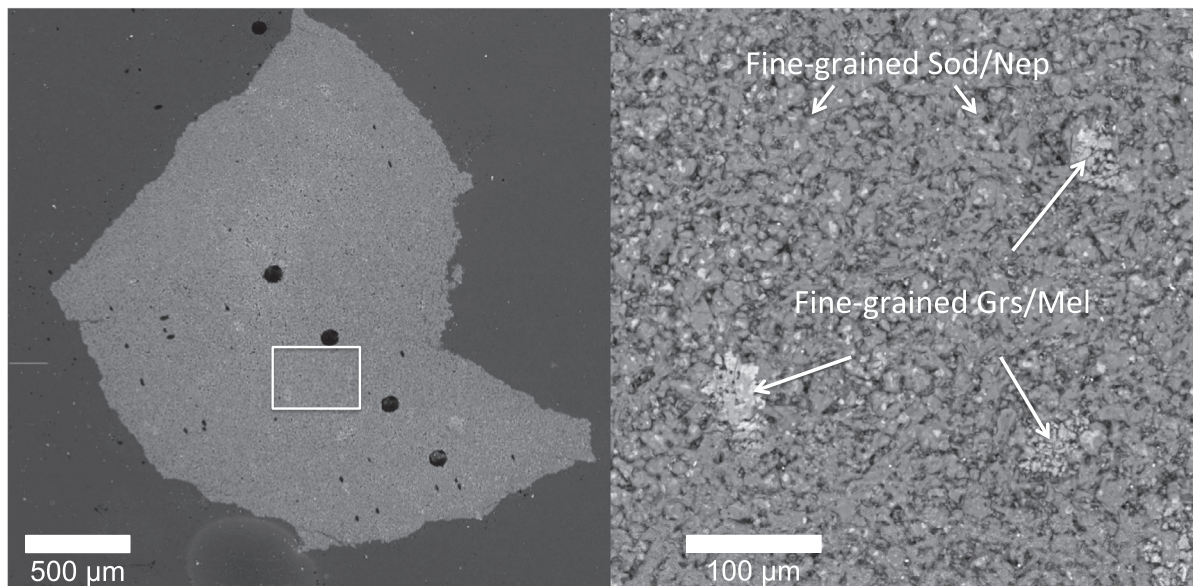


Fig. 1. Backscattered electron images of the *Curious Marie* CAI. The region outlined in panel (A) is shown in greater detail in panel (B). Fine-grained sodalite and nepheline are widely distributed in this heavily altered CAI with a small amount of grossular and melilite. The large dark circles in panel A result from prior laser ablation analyses. Mineral names: sod = sodalite; nep = nepheline; grs = grossular; mel = melilite.

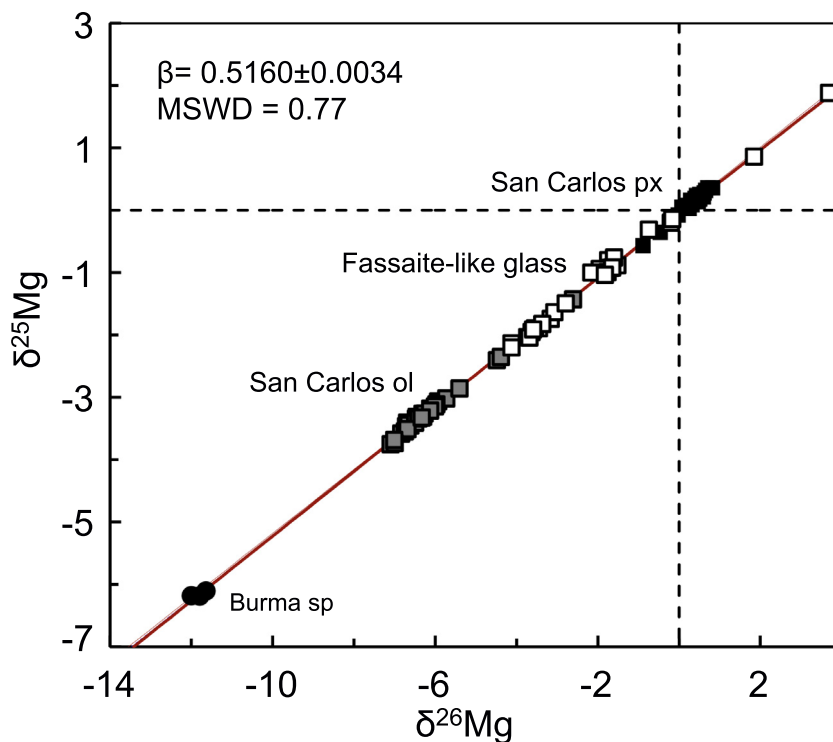


Fig. 2. The instrumental mass fractionation curve for Mg isotopes obtained from measurements of standards San Carlos olivine and diopside, Burma spinel and a synthetic glass of fassaite composition. A precise value of 0.5160 ± 0.0034 is calculated for instrumental mass fractionation factor (β) by linear regression using Isoplot 4.1 (Ludwig, 2012).

for charge compensation. The intensities of $^{16}\text{O}^-$ and $^{18}\text{O}^-$ were simultaneously measured with off-axis FC detectors (L2' and H1), whereas $^{17}\text{O}^-$ signals were measured with the axial EM. The mass resolving power (MRP) for ^{17}O was set at ~ 7000 so that the OH^- interference on $^{17}\text{O}^-$ could be sufficiently resolved. All the data were corrected for instrumental mass fractionations by using a piece of NIST 610 glass ($\delta^{17}\text{O} = 5.5\text{‰}$, $\delta^{18}\text{O} = 10.9\text{‰}$, Kasemann et al., 2001). The matrix effects on the instrumental mass fractionation (IMF) between NIST 610 glass and the analyzed Fe-poor phases are likely no more than a few permil/amu and are strictly mass dependent (Kita et al., 2010; Isa et al., 2016).

Negative S and Cl secondary ions were produced by a 0.6 nA Cs^+ primary ion beam focused to a $<10\ \mu\text{m}$ spot, and were measured with the axial EM in peak jumping mono-collection mode, with the mass sequence of 32.8, ^{33}S , ^{34}S , ^{35}Cl , ^{36}S and ^{37}Cl . A long pre-sputtering time was required (>20 min) to minimize surface S contamination. A mass resolving power of 5000 was used to resolve interferences (e.g., $^{32}\text{SH}^-$ and $^{35}\text{ClH}^-$) from the peaks of interest. Special attention was paid to characterizing the mass spectrum at mass 36. Typical count rates of ^{36}S from the sodalite in the CAI sample were 4–10 cps, much higher than background contributions from the noise in the ion counting system and/or in the mass spectrum (0.003 \sim 0.008 cps). The transmission was deliberately decreased to minimize the QSA effect (Quasi-Simultaneous Arrival, Slodzian et al., 2004) when measuring the pyrite

and troilite standards; data were corrected for a dead time of 65 ns. Sulfur isotopic ratios were calculated by using total counts due to the relatively low ^{36}S count rate (~ 3 – 10 cps; Ogiore et al., 2011). A systematic offset of $\sim 17\text{‰}$ on the $^{36}\text{S}/^{34}\text{S}$ ratio was observed on all the standards when normalizing the measured $^{36}\text{S}/^{34}\text{S}$ ratio to that of CDT ($^{36}\text{S}/^{34}\text{S}_{\text{CDT}} = 0.0034713$; Ding et al., 2001). This could result from the uncertain $^{36}\text{S}/^{34}\text{S}$ ratio in Canyon Diablo troilite. Therefore, to compensate for this 17‰ offset on the $^{36}\text{S}/^{34}\text{S}$ ratio, we normalized all the measured $^{36}\text{S}/^{34}\text{S}$ ratios to 0.0034147. The excesses of ^{36}S ($\equiv \delta^{36}\text{S}^*$) were calculated by fixing the $^{33}\text{S}/^{34}\text{S}$ ratio to the constant value of 0.17837 ratio using a linear law with a mass fractionation exponent of -0.481 obtained from standards (e.g., Balmat pyrite, Canyon Diablo troilite, and CAR 123 pyrite, Fig. 3). Because of the large uncertainties relative to the magnitude of the mass fractionation, the choice of mass fractionation law (e.g., linear vs. exponential) is irrelevant in this case for the calculation of $\delta^{36}\text{S}^*$. The calculation is as follows,

$$\delta^{36}\text{S}^* = \delta^{36}\text{S} - \left(\frac{\delta^{33}\text{S}}{-0.481} \right) \quad (1)$$

where

$$\delta^i\text{S} = \left[\frac{(^i\text{S}/^{34}\text{S})_{\text{measured}}}{0.0034147} - 1 \right] \times 1000 \quad (2)$$

and the error of $(^i\text{S}/^{34}\text{S})_{\text{measured}}$ was calculated by following an error-propagation equation,

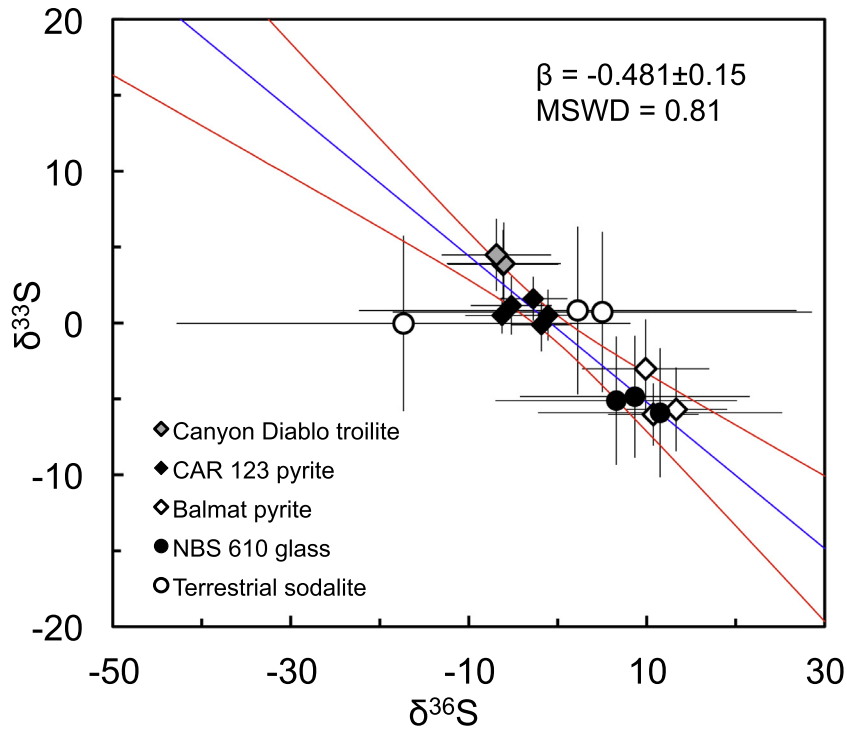


Fig. 3. The instrumental mass fractionation factor for the S isotopes obtained from standards Balmat pyrite, Canyon Diablo troilite, and CAR 123 pyrite. NIST glass 610 and a terrestrial sodalite are also plotted on the $\delta^{36}\text{S}$ - $\delta^{33}\text{S}$ mass fractionation line to monitor the analytical accuracy. β is determined to be -0.481 ± 0.150 by linear regression using Isoplot 4.1 (Ludwig, 2012).

$$\sigma(^i\text{S}/^{34}\text{S})_{\text{measured}} = \sqrt{\frac{1}{N_{i\text{S}}} + \frac{1}{N_{^{34}\text{S}}}} \times \frac{i\text{S}}{^{34}\text{S}} \quad (3)$$

in which $N_{i\text{S}}$ is the total counts of $i\text{S}$ and the error on $N_{i\text{S}}$ follows Poisson's law. Using this expression, the errors of $\delta^i\text{S}$ and $\delta^{36}\text{S}^*$ are calculated as follows,

$$\sigma(\delta^i\text{S}) = \frac{\sigma(^i\text{S}/^{34}\text{S})}{0.0034147} \times 1000 \quad (4)$$

and $\sigma(\delta^{36}\text{S}^*) = \sqrt{\sigma(\delta^{36}\text{S})^2 + \sigma(\delta^{33}\text{S})^2/0.481^2}$ terrestrial sodalite ($^{35}\text{Cl}/^{34}\text{S} \sim 15,000$) was measured to monitor the accuracy of the measured ^{36}S excess.

We estimated the bulk $^{35}\text{Cl}/^{34}\text{S}$ ratio of *Curious Marie* by sputtering thirty $25 \mu\text{m} \times 25 \mu\text{m}$ raster squares on the sample and then averaging the measured $^{35}\text{Cl}/^{34}\text{S}$ ratios. The signals of $^{32}\text{S}^-$ and $^{35}\text{Cl}^-$ were simultaneously collected with L1 (EM) and H2' (FC) under the mass resolving power of ~ 5000 . The $^{35}\text{Cl}/^{34}\text{S}$ ratio of each raster crater therefore can be calculated with the following equation,

$$\frac{^{35}\text{Cl}}{^{34}\text{S}} = \left(\frac{^{35}\text{Cl}}{^{32}\text{S}} \right)_{\text{measured}} \cdot \frac{^{32}\text{S}}{^{34}\text{S}} \cdot A_{^{35}\text{Cl}/^{34}\text{S}} \quad (5)$$

where $^{32}\text{S}/^{34}\text{S} = 22.57$. The relative sensitivity factor [RSF, $A_{^{35}\text{Cl}/^{34}\text{S}} \equiv (^{35}\text{Cl}/^{34}\text{S})_{\text{true}} / (^{35}\text{Cl}^- / ^{34}\text{S}^-)_{\text{measured}}$] of $^{35}\text{Cl}/^{34}\text{S}$ (~ 0.83) used throughout this study was determined from a NIST 610 glass ($\text{Cl}/\text{S} \sim 0.66$; Jochum et al., 2011).

3. RESULTS

The bulk analysis of REE concentrations performed via ICP-MS reveals that *Curious Marie* is characterized by a Group II REE pattern (Tissot et al., 2016), indicative of condensation of the CAI precursor in a reservoir in which the most refractory REEs had been previously depleted and the more volatile REEs were incompletely condensed (Boynnton, 1975; Davis and Grossman, 1979). The oxygen isotopic compositions in the secondary minerals of *Curious Marie* follow a mass-dependent fractionation line with $\Delta^{17}\text{O} = -8\text{‰}$ (Fig. 4A), similar to compositions obtained from secondary phases in other fine-grained CV CAIs (Aléon et al., 2005; Ushikubo et al., 2007).

The magnesium isotopic compositions measured in 9 spots of *Curious Marie* reveal excesses of $\delta^{26}\text{Mg}^*$ that are not correlated with $^{27}\text{Al}/^{24}\text{Mg}$ (Table 1 and Fig. 4B). Unlike sodalite and nepheline in other altered CAIs from Allende that showed close to terrestrial Mg isotopic compositions (open squares in Fig. 4B; data from Lin et al., 2005; Fagan et al., 2007; Ushikubo et al., 2007), all the spots in *Curious Marie* are characterized by a relatively uniform, yet elevated $\delta^{26}\text{Mg}^* = 43 \pm 6\text{‰}$ (2σ error, reduced $\chi^2 = 3$) over a large range of $^{27}\text{Al}/^{24}\text{Mg}$ ratio (from 50 to 800). The mass-dependent fractionation ($\delta^{25}\text{Mg}$) of the measured phases ranges from $\sim -7\text{‰}$ to -17‰ per amu, which is consistent with a condensation origin of the CAI precursor. Although the uniform ^{26}Mg excess independent of Al/Mg precludes the determination of an isochron, a model initial

$^{26}\text{Al}/^{27}\text{Al}$ ratio = $(6.2 \pm 0.9) \times 10^{-5}$ can still be inferred from the bulk $^{27}\text{Al}/^{24}\text{Mg}$ ratio (~ 95 , measured by solution ICPMS; Tissot et al., 2016) and assuming $\delta^{26}\text{Mg}_0 = 0$.

Results of Cl-S isotopic analyses in sodalite from *Curious Marie* are shown in Table 1 and Fig. 4C. Significant excesses in ^{36}S are clearly resolved over a large range of $^{35}\text{Cl}/^{34}\text{S}$ values (from 500 to 20,000). However, the ^{36}S excesses are uniformly elevated, with a weighted average of $97 \pm 12\%$ (2σ error, reduced $\chi^2 = 3$), independent of the Cl/S ratio, indicating late homogenization of the ^{36}S excesses after

^{36}Cl became extinct. The $^{35}\text{Cl}/^{34}\text{S}$ bulk ratio of *Curious Marie* was estimated as 935 ± 240 by averaging 30 raster analyses each comprising a $25 \mu\text{m} \times 25 \mu\text{m}$ surface area. The $^{36}\text{Cl}/^{35}\text{Cl}$ ratio at the time when the ^{36}Cl - ^{36}S system was closed can be constrained by applying the following equation,

$$\frac{^{36}\text{S}}{^{34}\text{S}_{\text{sample}}} = \frac{^{36}\text{Cl}}{^{35}\text{Cl}_t} \cdot \frac{^{35}\text{Cl}}{^{34}\text{S}_{\text{sample}}} \cdot 0.019 \quad (6)$$

where the 0.019 factor corresponds to the branching ratio of ^{36}Cl into ^{36}S . In this way, we estimate that bulk $^{36}\text{Cl}/^{35}\text{Cl}$ ratio of *Curious Marie* was $(2.3 \pm 0.6) \times 10^{-5}$. The uncertainty estimate given here does not include possible systematic errors due to any inhomogeneity in the NIST 610 glass used for calibrating the RSF of the glass and that of the mineral assemblages in *Curious Marie*. Nevertheless, this ratio is lower than the initial $^{36}\text{Cl}/^{35}\text{Cl}$ ratio in ESS inferred from previous studies on sodalites in other CAIs by a factor of 3–10 (Lin et al., 2005; Hsu et al., 2006) which is almost certainly outside of any possible systematic error.

4. DISCUSSION

4.1. ^{26}Al - ^{26}Mg systematics in *Curious Marie* CAI: evidence for early aqueous alteration

The negative mass-dependent Mg isotope fractionation found in *Curious Marie* suggests that this inclusion condensed from the early solar nebula without experiencing significant later evaporation events as evaporation tends to drive the residue towards heavy isotopic compositions (e.g., Mendybaev et al., 2013). The oxygen isotopic compositions in the secondary minerals of *Curious Marie* CAI are mass-dependently fractionated with a uniform $\Delta^{17}\text{O}$ value of -8% (Fig. 4A), comparable to the secondary phases found in other typical fine-grained CAIs (Clayton and

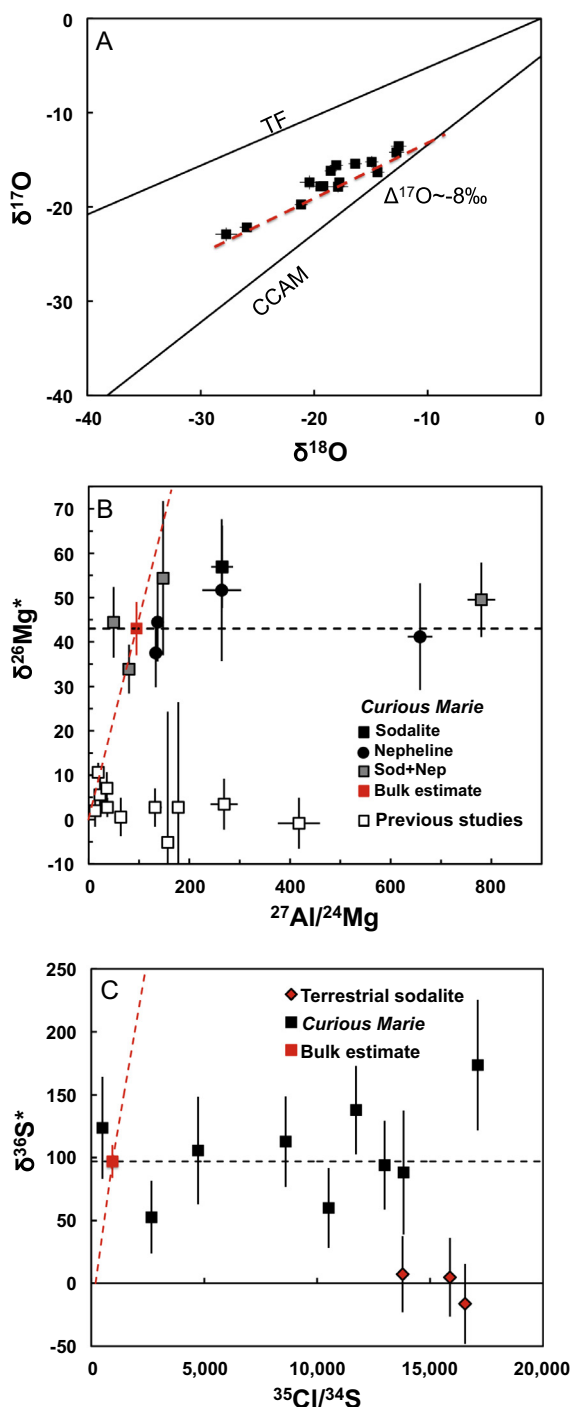


Fig. 4. (A) Oxygen isotopic compositions in the secondary phases of *Curious Marie* CAI follow a mass-dependent fractionation line with $\Delta^{17}\text{O}$ of -8% . (B) $^{26}\text{Mg}^*$, expressed in delta-notation, as a function of $^{27}\text{Al}/^{24}\text{Mg}$ measured in the secondary phases of *Curious Marie* CAI (black rectangle: sodalite; black circle, nepheline; gray rectangle: mixture of sodalite and nepheline) compared to previous analysis in other CAI sodalite (open squares, data are selected from Lin et al., 2005; Fagan et al., 2007; Ushikubo et al., 2007). An elevated and uniform ^{26}Mg excess ($\delta^{26}\text{Mg}_{\text{average}} = 43 \pm 6\%$, black dash line) was observed with $^{27}\text{Al}/^{24}\text{Mg}$ ranging from 50 to 800. According to the bulk elemental measurement ($^{27}\text{Al}/^{24}\text{Mg} = 95$, red square), an initial $^{26}\text{Al}/^{27}\text{Al}$ model ratio of $(6.2 \pm 0.9) \times 10^{-5}$ (red dash line) is calculated. (C) $^{36}\text{S}^*$, expressed as a delta-value, as a function of $^{35}\text{Cl}/^{34}\text{S}$ in sodalite of *Curious Marie* CAI (black squares). ^{36}S excesses are uniformly elevated, with a weighted average of $97 \pm 12\%$ independent of the $^{35}\text{Cl}/^{34}\text{S}$ ratios (black dash line), which range from 500 to 20,000. An initial $^{36}\text{Cl}/^{35}\text{Cl}$ model ratio of $(2.3 \pm 0.6) \times 10^{-5}$ (red dash line) is obtained based on the estimate on the bulk elemental ratio ($^{35}\text{Cl}/^{34}\text{S} = 935 \pm 240$, red square). Results from analysis of a terrestrial sodalite (red diamonds) are also plotted on panel (C) to ascertain the analytical accuracy. (For interpretation of the references to color in this figure legend, the reader is referred to the web version of this article.)

Table 1
Oxygen isotopic composition, Al-Mg and Cl-S systematics in the terrestrial standards and *Curious Marie* CAI.^a

Oxygen	$\delta^{17}\text{O}$ (‰)	$\delta^{18}\text{O}$ (‰)	$\Delta^{17}\text{O}$ (‰)
<i>Terrestrial standards</i>			
San Carlos Olivine	2.6 ± 0.4	4.9 ± 0.7	0.1 ± 0.5
	2.8 ± 0.4	5.9 ± 0.7	-0.3 ± 0.5
	3.0 ± 0.4	5.2 ± 0.7	0.4 ± 0.6
	2.7 ± 0.4	5.4 ± 0.7	-0.1 ± 0.5
Average	2.8 ± 0.7	5.3 ± 1.7	0.0 ± 1.0
NIST NBS 610	6.2 ± 0.3	11.2 ± 0.8	0.4 ± 0.5
	5.8 ± 0.6	11.8 ± 0.7	-0.4 ± 0.7
	5.7 ± 0.6	10.4 ± 0.9	0.3 ± 0.7
	5.3 ± 0.4	11.0 ± 0.8	-0.4 ± 0.6
	4.7 ± 0.5	10.2 ± 0.9	-0.6 ± 0.7
Average	5.6 ± 1.6	10.9 ± 1.7	-0.1 ± 1.2
<i>Curious Marie</i>			
Sodalite #1	-22.9 ± 0.7	-27.8 ± 1.0	-8.5 ± 0.9
Sodalite #2	-15.6 ± 0.4	-18.1 ± 0.6	-6.2 ± 0.5
Sodalite #3	-22.2 ± 0.5	-25.9 ± 0.6	-8.7 ± 0.6
Sodalite #4	-16.2 ± 0.4	-18.6 ± 0.5	-6.5 ± 0.5
Sodalite #5	-17.4 ± 0.7	-20.4 ± 0.9	-6.8 ± 0.9
Sodalite #6	-17.8 ± 0.4	-19.2 ± 0.4	-7.8 ± 0.4
Sodalite #7	-15.4 ± 0.5	-16.4 ± 0.6	-6.9 ± 0.6
Sodalite #8	-17.8 ± 0.4	-19.4 ± 0.6	-7.7 ± 0.5
Sodalite #9	-19.7 ± 0.4	-21.2 ± 0.6	-8.7 ± 0.5
²⁶ Al- ²⁶ Mg systematics	²⁷ Al/ ²⁴ Mg	F(Mg) (‰/amu)	$\delta^{26}\text{Mg}^*$ (‰)
<i>Terrestrial standards</i>			
Madagascar hibonite	44.5 ± 1.4	0.2 ± 1.4	0.4 ± 2.2
	44.7 ± 1.4	-0.6 ± 1.4	2.0 ± 2.2
	42.4 ± 1.3	-0.3 ± 1.2	1.0 ± 1.8
	42.3 ± 1.3	-0.4 ± 1.6	1.6 ± 2.6
	42.0 ± 1.2	-1.4 ± 1.3	0.0 ± 2.1
	42.3 ± 1.3	-0.1 ± 1.6	2.0 ± 2.5
	42.0 ± 1.3	1.2 ± 1.6	0.1 ± 2.4
	41.9 ± 1.3	1.1 ± 2.5	-1.8 ± 4.1
	42.1 ± 1.3	0.3 ± 1.7	2.8 ± 2.7
	Average	42.7 ± 0.7	0.0 ± 1.3
<i>Curious Marie</i>			
Sodalite #1	265.4 ± 22.3	-12.3 ± 2.9	56.9 ± 9.3
Nepheline #1	133.2 ± 5.1	-12.2 ± 2.5	37.5 ± 7.7
Nepheline #2	264.4 ± 39.0	-11.2 ± 5.1	51.7 ± 16.0
Nepheline #3	137.3 ± 8.1	-15.5 ± 2.7	44.5 ± 8.9
Nepheline #4	657.9 ± 23.5	-10.6 ± 3.7	41.2 ± 12.0
Sodalite + Nepheline #1	48.6 ± 5.2	-12.0 ± 2.6	44.4 ± 7.9
Sodalite + Nepheline #2	80.1 ± 2.0	-7.1 ± 1.8	33.9 ± 5.5
Sodalite + Nepheline #3	147.7 ± 5.3	-16.7 ± 5.1	54.4 ± 17.4
Sodalite + Nepheline #4	780.1 ± 26.7	-10.9 ± 2.7	49.5 ± 8.4
Weighted Average	95 ^b		42.7 ± 5.8
Average with 95% confidence			46.0 ± 12.6
³⁶ Cl- ³⁶ S systematics	³⁵ Cl/ ³⁴ S	³⁶ S/ ³⁴ S	$\delta^{36}\text{S}^*$ (‰) ^c
<i>Terrestrial standards</i>			
Terrestrial sodalite	16247	0.003432 ± 0.000106	5 ± 31
	16928	0.003360 ± 0.000109	-16 ± 32
	14098	0.003439 ± 0.000102	7 ± 30
Average	15758	0.003116 ± 0.000133	-1 ± 39

(continued on next page)

Table 1 (continued)

Oxygen	$\delta^{17}\text{O}$ (‰)	$\delta^{18}\text{O}$ (‰)	$\Delta^{17}\text{O}$ (‰)
<i>Curious Marie</i>			
Sodalite #1	12164	0.003886 ± 0.000120	138 ± 35
Sodalite #2	14351	0.003715 ± 0.000167	88 ± 49
Sodalite #3	17758	0.004009 ± 0.000178	174 ± 52
Sodalite #4	4836	0.003777 ± 0.000147	106 ± 43
Sodalite #5	2725	0.003596 ± 0.000099	53 ± 29
Sodalite #6	509	0.003838 ± 0.000140	124 ± 41
Sodalite #7	13283	0.003736 ± 0.000120	94 ± 35
Sodalite #8	8804	0.003801 ± 0.000123	113 ± 36
Sodalite #9	10750	0.003620 ± 0.000109	60 ± 32
Weighted average	$935 \pm 240^{\text{d}}$	0.003746 ± 0.000044	97 ± 12

^a The uncertainties are referred to 2 S.E.

^b The bulk $^{27}\text{Al}/^{24}\text{Mg}$ in *Curious Marie* was obtained from ICP-MS measurement in Tissot et al. (2016).

^c $\delta^{36}\text{S}^*$ values are normalized to $^{36}\text{S}/^{34}\text{S} = 0.0034147$ (see the text for interpretation).

^d The bulk $^{35}\text{Cl}/^{34}\text{S}$ in *Curious Marie* is estimated by the average of *in situ* analyses on $^{35}\text{Cl}/^{34}\text{S}$ ratio.

Mayeda, 1984; Rowe et al., 1994; Aléon et al., 2005; Ushikubo et al., 2007). In addition, bulk measurements of the titanium isotopic composition of *Curious Marie* showed no significant mass-dependent fractionation ($F_{\text{Ti}} = -0.2 \pm 0.1\%$) and a typical ^{50}Ti isotopic anomaly, $\epsilon^{50}\text{Ti} = +8.9 \pm 0.3$ (see Supplement online material of Tissot et al., 2016). In general, *Curious Marie* has the stable isotopic characteristics of a typical unmelted fine-grained Allende CAI except that it is pervasively altered and it is rich in secondary phases.

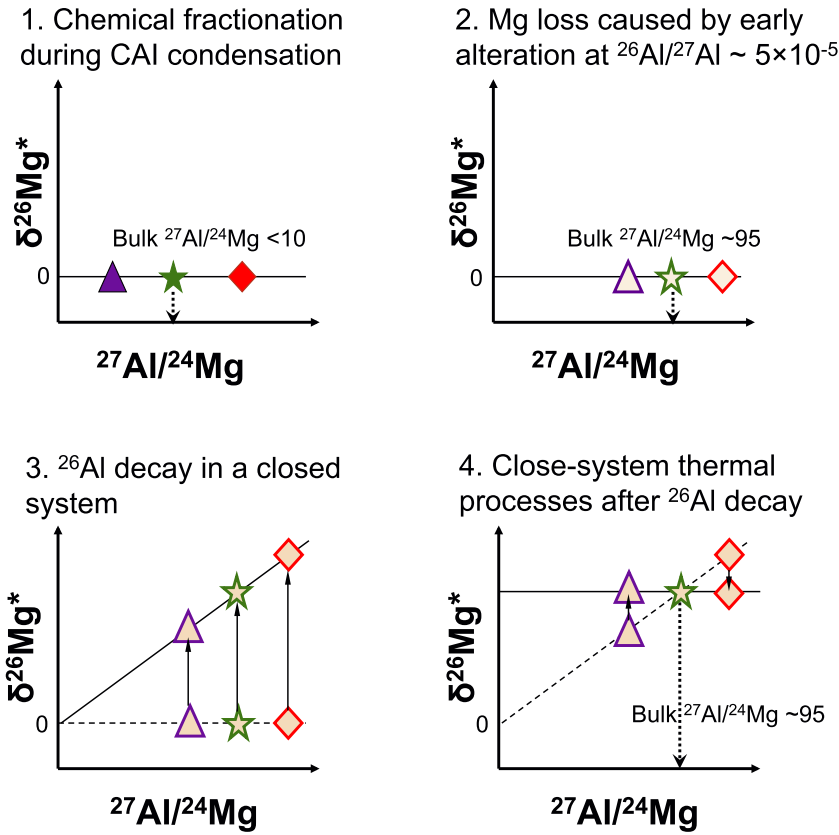
The Al-Mg systematics in the secondary phases of CAIs can be used to constrain the chronology of the alteration processes. In general, these secondary phases in most CAIs are characterized by disturbed Mg isotopic compositions, from which only very low or zero initial $^{26}\text{Al}/^{27}\text{Al}$ ratios can be derived (Hutcheon and Newton, 1981; Lin et al., 2005; Fagan et al., 2007; Ushikubo et al., 2007). This is often attributed to late aqueous alteration events in which Mg isotopic exchange between a CAI and an external fluid leads to a loss of radiogenic ^{26}Mg excesses after ^{26}Al has decayed away (Hutcheon and Newton, 1981; Lin et al., 2005; Fagan et al., 2007; Ushikubo et al., 2007; Krot et al., 2010). In contrast to this pattern, we find a uniform ^{26}Mg excess of average value $+43 \pm 6\%$ all throughout the *Curious Marie* CAI with an elevated bulk $^{27}\text{Al}/^{24}\text{Mg}$ ratio (~ 95). Since *Curious Marie* is a typical fine-grained CAI, and not a FUN inclusion, it is safe to assume that this ^{26}Mg excess is a radiogenic product from the decay of ^{26}Al instead of a nucleosynthetic signature. We calculate a model $^{26}\text{Al}/^{27}\text{Al}$ ratio of $(6.2 \pm 0.9) \times 10^{-5}$, which is consistent with the canonical value $((5.27 \pm 0.17) \times 10^{-5}$, Jacobsen et al., 2008; MacPherson et al., 2010) within uncertainties. Thus, the *Curious Marie*'s precursor could have formed contemporaneously with other large CV3 CAIs that carry canonical $^{26}\text{Al}/^{27}\text{Al}$. The elevated homogeneous ^{26}Mg excess in the secondary phases therefore indicates isotopic homogenization without contamination with chondritic Mg. Al-Mg systematics in the secondary phases of *Curious Marie* may thus constrain the timing of this alteration event.

The survival of a canonical $^{26}\text{Al}/^{27}\text{Al}$ ratio in *Curious Marie* means that ^{26}Mg loss during aqueous alteration, if it happened, must have been very limited. This is inconsistent with open-system aqueous alteration occurring after significant decay of ^{26}Al to generate secondary minerals including sodalite and nepheline, as that would lead to large Mg loss (including ^{26}Mg) and elevated Al/Mg ratios, and thereby result in a model initial $^{26}\text{Al}/^{27}\text{Al}$ ratio much lower than the canonical value. To preserve the canonical model initial $^{26}\text{Al}/^{27}\text{Al}$ ratio in the intensely altered *Curious Marie*, while losing enough Mg to offset the bulk $^{27}\text{Al}/^{24}\text{Mg}$ from a relatively low value ($^{27}\text{Al}/^{24}\text{Mg} = 2\text{--}10$ in Allende CAIs that show no to little signs of alteration, e.g., Galy et al., 2000; Thrane et al., 2006; Jacobsen et al., 2008; Larsen et al., 2011) to ~ 95 , aqueous alteration and the formation of sodalite and nepheline must have taken place when ^{26}Al was still extant. Due to the absence of radiogenic ^{26}Mg at the time of this early alteration, the open-system reactions only re-distributed the primordial Mg isotopes. Therefore, the evolution of ^{26}Al - ^{26}Mg systematics in secondary phases remained undisturbed and resulted in a model initial $^{26}\text{Al}/^{27}\text{Al}$ ratio of $\sim 5 \times 10^{-5}$ (Fig. 5). The homogeneous $\delta^{26}\text{Mg}^*$ further implies that after ^{26}Al had completely decayed away, Mg isotopes were then homogenized through closed-system thermal processing.

As shown in Fig. 5, an upper limit on the time interval between the condensation of the precursors of *Curious Marie* and early alteration can be estimated by considering a two-stage model. Assuming that the condensation of precursors minerals of *Curious Marie* and the early alteration occurred at t_0 and t_1 , respectively, the ^{26}Mg excess in the precursors at time t_1 can be calculated as follows,

$$\frac{^{26}\text{Mg}}{^{24}\text{Mg}_{t_1}} = \frac{^{26}\text{Mg}}{^{24}\text{Mg}_{t_0}} + \frac{^{26}\text{Al}}{^{27}\text{Al}_{t_0}} \frac{^{27}\text{Al}}{^{24}\text{Mg}_{t_0}} [1 - e^{-\lambda(t_1-t_0)}] \quad (7)$$

At time t_1 , secondary phases were produced by aqueous alteration, leading to fractionation of the $^{27}\text{Al}/^{24}\text{Mg}$ ratio in *Curious Marie* from $\sim 2\text{--}10$ to ~ 95 . If the entire system stayed closed after this alteration, the present ^{26}Mg excess



$^{26}\text{Al}/^{26}\text{Mg}$ systematics in *Curious Marie*

Fig. 5. Schematic diagram of Al-Mg systematics in *Curious Marie* CAI. The bulk $^{27}\text{Al}/^{24}\text{Mg}$ ratio of the precursor was 0–10 at Solar System formation. Then this CAI experienced alteration involving external fluids when ^{26}Al was at the canonical value. In this process, the initial Mg was washed away, resulting in a higher $^{27}\text{Al}/^{24}\text{Mg}$ ratio (~ 95). Besides, due to the absence of radiogenic ^{26}Mg during this extremely early alteration, the ^{26}Al - ^{26}Mg systematics stayed “undisturbed”, leading to an internal isochron with $^{26}\text{Al}/^{27}\text{Al}$ ratio $\sim 5 \times 10^{-5}$ among the secondary phases. After ^{26}Al extinction, Mg isotopic compositions were homogenized in close-system thermal processes on the chondrite parent body, offering a model initial $^{26}\text{Al}/^{27}\text{Al}$ ratio $\sim 5 \times 10^{-5}$ in the bulk sample and uniform and elevated radiogenic ^{26}Mg excesses among different phases.

in the secondary phases can be calculated using the following equation,

$$\begin{aligned} \frac{^{26}\text{Mg}}{^{24}\text{Mg}}_{\text{present}} &= \frac{^{26}\text{Mg}}{^{24}\text{Mg}}_{t_1} + \frac{^{26}\text{Al}}{^{27}\text{Al}}_{t_1} \frac{^{27}\text{Al}}{^{24}\text{Mg}}_{t_1} \\ &= \frac{^{26}\text{Mg}}{^{24}\text{Mg}}_{t_1} + \frac{^{26}\text{Al}}{^{27}\text{Al}}_{t_0} e^{-\lambda(t_1-t_0)} \frac{^{27}\text{Al}}{^{24}\text{Mg}}_{t_1} \end{aligned} \quad (8)$$

In $\delta^{26}\text{Mg}$ notation, this takes the form,

$$\begin{aligned} \delta^{26}\text{Mg}_{\text{present}} &= \delta^{26}\text{Mg}_{t_0} + \frac{^{26}\text{Al}}{^{27}\text{Al}}_{t_0} \\ &\times \left[\frac{\frac{^{27}\text{Al}}{^{24}\text{Mg}}_{t_1} - \frac{^{27}\text{Al}}{^{24}\text{Mg}}_{t_0} e^{-\lambda(t_1-t_0)} + \frac{^{27}\text{Al}}{^{24}\text{Mg}}_{t_1} e^{-\lambda(t_1-t_0)}}{\frac{^{26}\text{Mg}}{^{24}\text{Mg}}_{\text{standard}}} \right] \\ &\times 10^3 \end{aligned} \quad (9)$$

in which $t_0 = 0$ Myr at CAI condensation, the primordial ^{26}Mg isotopic composition $\delta^{26}\text{Mg}_{t_0} = 0\%$, $\frac{^{26}\text{Mg}}{^{24}\text{Mg}}_{\text{standard}} = 0.13932$ and $\frac{^{26}\text{Al}}{^{27}\text{Al}}_{t_0} = (5.27 \pm$

$0.17) \times 10^{-5}$. The bulk $^{27}\text{Al}/^{24}\text{Mg}$ ratio at t_1 in *Curious Marie* is the presently determined value of 95. The bulk $\delta^{26}\text{Mg}^*$ value in *Curious Marie* is $46.0 \pm 12.6\%$ (Table 1). The bulk $^{27}\text{Al}/^{24}\text{Mg}_{t_0}$ ratio in the precursor of *Curious Marie* is conservatively estimated as 2–10 based on previous studies on unaltered CAIs (e.g., Galy et al., 2000; Thrane et al., 2006; Jacobsen et al., 2008; Larsen et al., 2011). Since the model $^{26}\text{Al}/^{27}\text{Al}$ ratio in *Curious Marie* is identical to the canonical ratio within the uncertainty, t_1 cannot be resolved through Eq. (9). However, by propagating the errors of $\frac{^{26}\text{Al}}{^{27}\text{Al}}_{t_0}$ and the bulk $\delta^{26}\text{Mg}^*$ in *Curious Marie* to t_1 , an upper limit of ~ 50 kyr can be constrained for the occurrence of early alteration after the condensation of *Curious Marie*.

According to previous observations in sodalites and other secondary minerals (see Fig. 4B; Hutcheon and Newton, 1981; Lin et al., 2005; Fagan et al., 2007; Ushikubo et al., 2007), the Cl-rich fluid involved in sodalite formation transported Na into the primary phases to

replace Ca and Mg. An analogy may be made with Mg transport from rocks to seawater. According to studies on sea-floor alteration, Mg extraction from rocks has been observed in widespread regions as a result of water-rock reactions at relatively low temperatures (0–100 °C), at high water/rock ratios (10^3 – 10^5), and in solutions undersaturated in Mg (Snow and Dick, 1995). This high mobility of Mg compared to Fe, Si, and Al in natural low-temperature water-rock reactions is consistent with experimental work on elemental mobility in mafic rocks during water-rock reactions that demonstrate that Mg and Ca have the highest mobility, followed by Fe, and Al (Anderson and Hawkes, 1958; Luce et al., 1972; Siever and Woodford, 1979; Schott et al., 1981). This mobility sequence is also revealed in *Curious Marie*, as both Ca and Mg are depleted: the bulk Ca/Al ratio of this CAI is ~ 0.08 (Tissot et al., 2016), at least three times lower than the ratios inferred from less altered fine-grained CAIs (Ca/Al ~ 0.25 – 0.67). The depletion of Ca and Mg relative to Al also provides evidence of the action of aqueous alteration involving an external fluid, which changed the chemistry of the primary phases and could have compromised the Al-Mg isotopic system (Krot et al., 2004). As discussed above, this must have taken place very early after solar system formation, in order to preserve the radiogenic ^{26}Mg in the bulk CAI.

The conditions of sodalite-forming aqueous alteration can be further constrained from the chemical characteristics in *Curious Marie*. The bulk uranium concentration of this CAI is only 5% of that in CI chondrites ($\text{U}/\text{U}_{\text{CI}} = 0.05$), whereas most CAIs are relatively enriched in U since it is refractory. Tissot et al. (2016) explain this extreme depletion as a result of intense aqueous alteration. Uranium behaves as a refractory element during CAI condensation in a reduced nebular gas, but it becomes mobile and soluble as U^{6+} when exposed to an oxidizing fluid (Langmuir, 1978; Wanner and Forest, 1992; Fruchter, 1998). The oxidizing fluid responsible for producing sodalite and nepheline would induce a substantial U loss.

The upper limit on the time of open-system alteration in *Curious Marie* provides a tight constraint on the timescale of Cm/U fractionation in the CAI. Tissot et al. (2016) analyzed the uranium isotopic composition in *Curious Marie* and other fine-grained Allende CAIs. From those measurements, they inferred a $^{247}\text{Cm}/^{235}\text{U}$ ratio of $(5.6 \pm 0.3) \times 10^{-5}$ at the time of Cm/U fractionation. Since the absolute time of this fractionation was unknown, the initial $^{247}\text{Cm}/^{235}\text{U}$ ratio in the ESS was estimated to be $(7.0 \pm 1.6) \times 10^{-5}$ by assuming that the fractionation occurred within the first 10 Myr of solar system formation. The present study shows that the canonical $^{26}\text{Al}/^{27}\text{Al}$ model ratio in *Curious Marie* requires an early aqueous alteration event, which presumably also fractionated the Cm/U ratio and generated secondary phases. Therefore, the age correction is minimal (compared to the 15.6 Myr half-life of ^{247}Cm) and the inferred $^{247}\text{Cm}/^{238}\text{U}$ ratio of $(5.6 \pm 0.3) \times 10^{-5}$ for *Curious Marie* should represent the best estimate for the initial ^{247}Cm abundance in the Solar System.

4.2. Aqueous alteration in a small precursor planetesimal with a canonical $^{26}\text{Al}/^{27}\text{Al}$ ratio

Textures indicative of nebular alteration with a vapor, such as euhedral wollastonite whiskers, nepheline needles, and grossular in cavities (Hashimoto and Grossman, 1987; Russell and MacPherson, 1997) are not observed in *Curious Marie*. Furthermore, the large U depletion and the wide distribution of sodalite and nepheline requires intense alteration involving an external fluid, suggesting alteration in a planetesimal instead of a nebular process.

With ~ 3 MeV per decay (Matson et al., 2009 and references therein), ^{26}Al is one of the most effective heat sources for thermal processing in an early accreted meteorite parent body. Numerical simulations (Herndon and Herndon, 1977; Hutcheon and Hutchison, 1989; Srinivasan et al., 1999; Young, 2001; Sahijpal et al., 2007) show that a large planetesimal (radius > 50 km) with high levels of ^{26}Al will differentiate due to radioactive heating, producing a basaltic melt that could exist over the first ~ 8 Myr of the ESS. This is consistent with ^{26}Al - ^{26}Mg and ^{53}Mn - ^{53}Cr chronologies in HED meteorites and angrites that indicate crust-mantle differentiation within the first 4 Myr after CAI (Srinivasan et al., 1999; Srinivasan, 2002; Nyquist et al., 2001, 2003a, 2003b; Baker et al., 2005; Sugiura et al., 2005; Markowski et al., 2006; Trinquier et al., 2008; Spivak-Birndorf et al., 2009; Schiller et al., 2010). On small planetesimals, a magma ocean would exist for at least the first hundreds of thousands of years, therefore preventing low temperature aqueous alteration of surface materials during this interval. Yet, we have argued above that the mineralogy and chronology of *Curious Marie* requires fluid-rock interactions on a parent body at an early time, when ^{26}Al abundance was near the canonical level, so we may ask how it is that such a sample could have experienced only relatively low temperature aqueous alteration on a parent body, without that body having melted and differentiated.

To address this issue, we modeled the thermal evolution of small parent bodies ($r = 2$ – 20 km) that accreted within the first 0.5 Myr after CAI. The goal is to understand the distribution of the areas with conditions suitable for sodalite and nepheline formation (hydrothermal temperature, 100–500 °C, Barrer and White, 1952; Veit et al., 1991) and Mg leaching from the rock (low temperature with liquid water, 0–100 °C; Snow and Dick, 1995) in such early-formed planetesimals. The thermal evolution of the planetesimals calculated here (described in detail in Zhou et al., 2013) was dominated by the competing effects of heat generated by the decay of ^{26}Al distributed homogeneously throughout the whole body (6.4×10^{-13} J per decay) and the enthalpies of reactions. The energy conservation equation is as follows,

$$\frac{\partial T}{\partial t} = \kappa \left(\frac{\partial^2 T}{\partial r^2} + \frac{2}{r} \frac{\partial T}{\partial r} \right) + (1 - \phi) \frac{Q}{C} \quad (10)$$

in which T is temperature, t is time, κ is the thermal conductivity of a rock, r is the radial distance from the center of

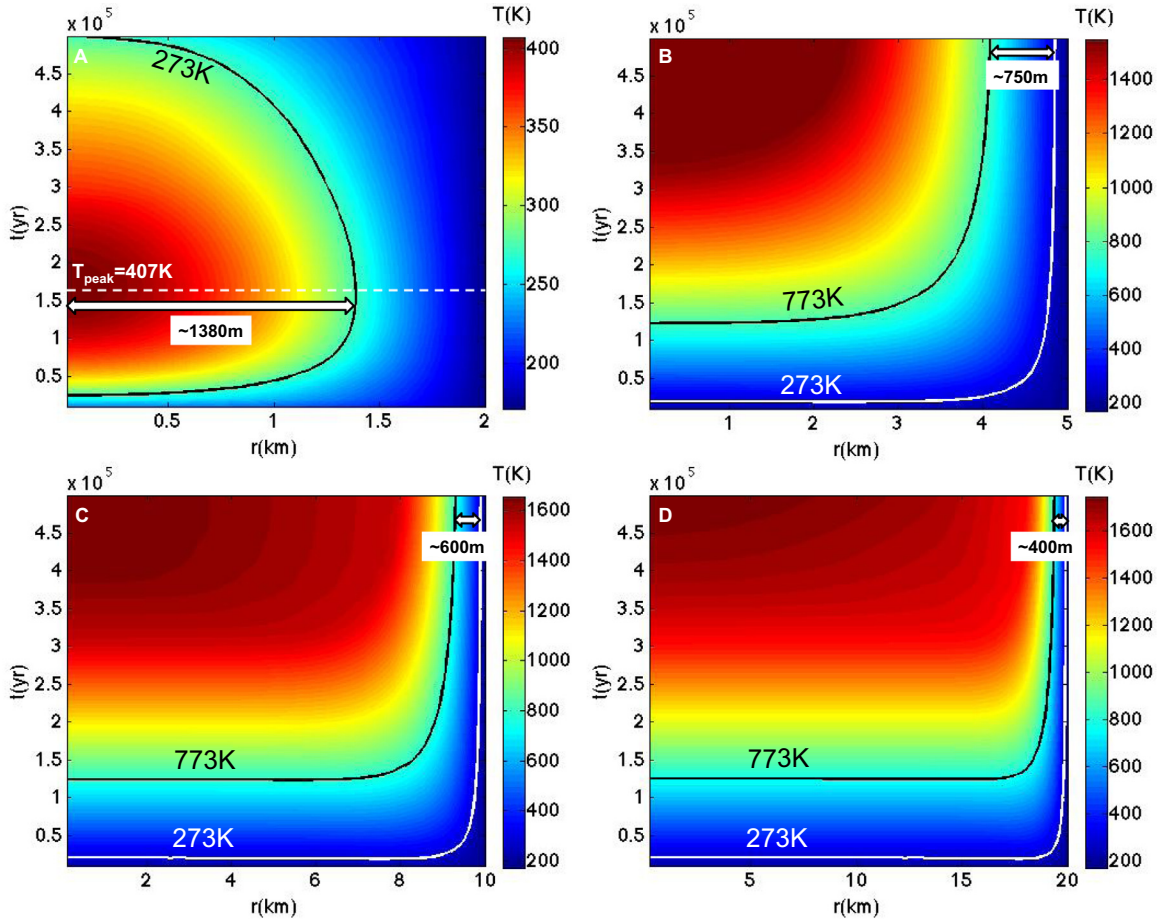


Fig. 6. Temperature distributions in the interior of a small icy body with the radius of 2 km (A), 5 km (B), 10 km (C), and 20 km (D) for their first 500 kyr following accretion. The volume fraction of water in all bodies is defined to be 20%. Parameters applied in this model follow Table 4 in Zhou et al. (2013). All the small bodies are assumed to have accreted rapidly when ^{26}Al was still at the canonical value ($t_{\text{accr}} \sim 0$ Ma). The peak temperature is achieved in 170 kyr in the 2 km body (407 K white dash line). The temperature contours of 273 K and 773 K are highlighted using bold curves. Within this area the temperature is appropriate for the potential water-rock interaction and hydrothermal processes. The minimum thickness of this area is estimated at the highest temperature, ranging from 1380 m to 400 m. Due to the decreasing proportion of this layer relative to the entire body with increasing radius of the planetesimals (see the text), we suggest that *Curious Marie* is highly likely to have been altered in the near surface fluid-rich layer on a small-size icy planetesimal before accretion onto the Allende parent body.

the body, ϕ is the volumetric fraction of the body composed of ice, Q is the energy produced through ^{26}Al decay per unit time, and C is the effective heat capacity of the rock. Assuming a CI abundance of Al, the heat production can be expressed in W kg^{-1} as $Q = 6 \times 10^{-3} ({}^{26}\text{Al}/{}^{27}\text{Al})_0 e^{(-\lambda t)}$ where λ is the decay constant of ^{26}Al , $({}^{26}\text{Al}/{}^{27}\text{Al})_0$ is the canonical value in the ESS, and t is the time after CAI condensation. *Curious Marie* is presumed to experience aqueous alteration on a small icy body with a limited gas permeability, and the bulk water content of the planetesimals is set to 8.3 wt% (20 vol%). More details on this model can be found in [Supporting Online Material](#).

Results for small planetesimals ($r = 2\text{--}20$ km) are shown in Fig. 6. Our calculations suggest that low-temperature aqueous alteration (0–100 °C) and hydrothermal events (100–500 °C) can take place near the surface of such objects within the first several hundred thousand years and that the duration of the heating event is mainly dependent on the

size of the bodies. For example, in a planetesimal with a 2 km radius, significant heating via ^{26}Al decay persists for only ~ 0.2 Myr and the core is not melted ($T_{\text{core}} < \sim 400$ K), whereas in bodies with a 20 km radius, thermal processing can last for more than 5 Myr with core temperatures reaching up to 1700 K. In this model, we consider that fluid flow occurs only at temperatures between 273 K (0 °C) and 773 K (500 °C) (black contours in Fig. 6). Even for planetesimals of very different sizes, the energy from ^{26}Al decay is sufficient to initiate hydrothermal processing rapidly within the first 40 kyr over the entire body except the frozen surface layer, and all planetesimal cores reach their peak temperatures within 500 kyr. Given that the decomposition temperature for the sodalite framework structure is ~ 1000 K (Veit et al., 1991), an altered carbonaceous chondrite rock, such as that containing *Curious Marie*, cannot have come from depths that reached this temperature but must have originated in the areas with persistent fluid flow,

that is between the 773 K and 273 K contours. From inspection of Fig. 6, it is clear that the size of this sub-surface region, relative to that of the entire body, is significantly reduced with increasing planetesimal radius. For example, on a 2 km radius planetesimal, fluids become active in the interior area from the first 20 kyr to 500 kyr, giving a volume proportion of 33% for the hydrothermal zone compared to the entire body. A similar proportion of 36% is obtained on a 5 km radius body. However, this proportion decreases to 17% and 6% on 10 km and 20 km radii planetesimals, respectively, because the fluid activity on such bodies is restricted within a narrower zone. Hence, intensely altered chondrite constituents, of which *Curious Marie* is an example, are more likely located in the outer part of an early accreted small icy body ($r < 10$ km).

Based on petrographic observations, Metzler, Bischoff and others have suggested that some components of aqueously altered (Type 1 and Type 2) carbonaceous chondrites were formed (and altered) in a previous generation(s) of planetesimals prior to incorporation into their current asteroidal parent bodies (Metzler et al., 1992; Bischoff, 1998). The scenario implied by our thermal models is consistent with the alteration of anhydrous silicates in relatively small and uncompacted planetesimals that accreted refractory inclusions, chondrules, fine-grained nebula condensates, and water ice (Metzler et al., 1992). Small planetesimals can subsequently be destroyed by collision, or explosively disrupted by vapor pressure from their interior (Wilson et al., 1998, 1999). As a result, various kinds of both altered or unaltered components could be re-accreted and incorporated into carbonaceous chondrite parent-bodies.

A large body of evidence exists for so-called “pre-accretionary alteration” in different carbonaceous chondrite groups (see review by Bischoff, 1998). Yet, for CV chondrites the existence of this process is debated (Cohen et al., 1983; Hashimoto and Grossman, 1987; Keller and Buseck, 1989; Jogo et al., 2009). Our study of *Curious Marie* provides strong support for the existence of an early generation of planetesimals that aqueously altered some of the material found in CV chondrites. The ice melted by ^{26}Al heating provided a fluid to alter the primary mineralogy of the CAI, while simultaneously leaching away uranium, increasing the $\Delta^{17}\text{O}$ value, and mobilizing Mg isotopes. After this early aqueous alteration, the pre-accretionary icy body carrying *Curious Marie* would have been disrupted and portions were incorporated into the CV parent planetesimal ($r > 200$ km) where they would mix with other chondritic components. Later thermal metamorphism

(Elkins-Tanton et al., 2011; Sahijpal and Gupta, 2011; Šrámek et al., 2012) could have led to homogenization of ^{26}Mg and ^{36}S excesses in *Curious Marie* (see below).

4.3. Late thermal processes in Allende parent body: Closed-system homogenization of ^{26}Mg and ^{36}S in *Curious Marie* CAI

The uniform ^{26}Mg and ^{36}S excesses in the secondary phases of *Curious Marie* require that some closed-system thermal processing took place in the CV parent body after the complete decay of ^{26}Al . The condition of the late thermal metamorphism can be constrained through the mineralogy and chemical composition of the host meteorite. The presence of ferrous olivine in the dark inclusions of Allende suggests extensive dehydration of phyllosilicates in the parent body (Kojima and Tomeoka, 1996) compared to the aqueously altered CM/CI chondrites (Krot et al., 1997). Based on the formation of nonporous rims around some of these dark inclusions (Buchanan et al., 1997), it has been estimated that the temperature of dehydration could have been as high as 600 °C (Krot et al., 1997). Thus, an important aspect to consider in assessing whether our proposed scenario is realistic is the duration required for isotopic homogenization of Mg and S in sodalite and nepheline at 600 °C. Although the self-diffusion coefficients for Mg and S in hydrous secondary minerals in meteorites are not available, we approximate them using the Mg diffusivity data in anorthite (LaTourrette and Wasserburg, 1998) because this mineral is one of the potential precursors for the feldspathoid minerals nepheline and sodalite (Sharp et al., 1989; Kimura and Ikeda, 1995). Given the small grain size of the secondary phases in *Curious Marie* (< 10 μm), ^{26}Mg excesses can be homogenized within a short time ($\sim 10^4$ years) at ~ 600 °C. We are not aware of any studies for sulfur thermal diffusivity in relevant mineral phases. Thus, we presume that sulfur isotope compositions in the secondary phases of *Curious Marie* CAI can be homogenized contemporaneously with Mg isotopes during metamorphism on the Allende parent body.

To sum up, in order to interpret our experimental results, *Curious Marie* must have experienced at least four stages of major events: (1) the precursor of *Curious Marie* condensed in the early solar nebula with other CAIs; (2) this precursor was rapidly transported beyond the snowline and accreted into a small icy body in which it was heavily altered by a NaCl-rich oxidizing fluid (carrying live ^{36}Cl) to form secondary phases such as sodalite and nepheline within ~ 50 kyr; (3) the small icy body was broken up and

Table 2
Summary of ^{26}Al - ^{26}Mg and ^{36}Cl - ^{36}S systematics in Cl-rich secondary phases of CAIs in this study and previous work.

CAI	Mineral	Reference	$^{26}\text{Al}/^{27}\text{Al}$	Age (Myr)	$^{36}\text{Cl}/^{35}\text{Cl}$	$^{36}\text{Cl}/^{35}\text{Cl}_{\text{initial}}$
Ningqiang CAI	Sodalite	Lin et al. (2005)	$\sim 1 \times 10^{-5}$	1.8	$\sim 5 \times 10^{-6}$	$\sim 2.9 \times 10^{-4}$
Pink Angel	Sodalite	Hsu et al. (2006)	$< 1.7 \times 10^{-6}$	> 3.6	$(3.7 \pm 0.8) \times 10^{-6}$	$> 1.6 \times 10^{-2}$
AJEF CAI	Wadalite	Jacobsen et al. (2011)	$(1.1 \pm 2.8) \times 10^{-6}$	≥ 4.1	$(1.8 \pm 0.1) \times 10^{-5}$	$\sim 2.2 \times 10^{-1}$
Allende Type B2 CAI	Sodalite	Ushikubo et al. (2007)	$< 4.4 \times 10^{-7}$	> 5.0	$(1.4 \pm 0.3) \times 10^{-6}$	$\sim 1.6 \times 10^{-1}$
Pink Angel	Sodalite	Nakashima et al. (2008)	$< 1.7 \times 10^{-6}$	> 3.6	$(1.8 \pm 2.2) \times 10^{-6}$	$> 7.7 \times 10^{-3}$
<i>Curious Marie</i>	Sodalite	This study	$(6.2 \pm 0.9) \times 10^{-5}$	< 0.2	$(2.3 \pm 0.6) \times 10^{-5}$	$1.7 \times 10^{-5} - 3 \times 10^{-5}$

a fragment carrying *Curious Marie* was accreted into the CV parent body; and (4) Mg and S isotopic compositions were homogenized by closed-system thermal processing after the extinction of ^{26}Al , within the CV parent asteroid. The duration of the heating event leading to isotopic homogenization is dependent on temperature but was on the order of $\sim 10^4$ years assuming a temperature of ~ 600 °C.

4.4. ^{36}Cl - ^{36}S systematics in *Curious Marie*: ^{26}Al and ^{36}Cl co-existed in the early solar nebula

The existence of ^{36}Cl in the secondary phases of chondrite constituents is thought to be a result of either late-stage solar energetic particle (SEP) irradiation of dust and gas near the proto-Sun, or injection into the early solar nebula from stellar sources such as supernovae, asymptotic giant branch stars or Wolf-Rayet stars (Leya et al., 2003; Goswami et al., 2005; Gounelle et al., 2006; Wasserburg et al., 2006). The calculated $^{26}\text{Al}/^{27}\text{Al}$ initial ratios in the chondrite constituents analyzed for ^{36}Cl in previous studies is $2\text{--}3 \times 10^{-6}$, implying that the secondary phases were formed at least ~ 3 Myr after CAI condensation. With this assumed timescale, ^{36}Cl - ^{36}S isotopic analyses on sodalite-rich alteration assemblages from Ningqiang CAI, Allende CAI, and a porphyritic chondrule suggest a minimum $^{36}\text{Cl}/^{35}\text{Cl}$ ratio of $\geq 1.6 \times 10^{-4}$ at the time of CAI formation (Lin et al., 2005; Hsu et al., 2006; Ushikubo et al., 2007).

Jacobsen et al. (2011) reported high initial $^{36}\text{Cl}/^{35}\text{Cl}$ ratios ($\sim 1.8 \times 10^{-5}$) from analyses of wadalite in the Allende CAI AJEF. These authors concluded that either ^{36}Cl was produced by SEP irradiation ~ 3 Myr after CAI formation, or that if ^{36}Cl and ^{26}Al were coeval then the initial $^{36}\text{Cl}/^{35}\text{Cl}$ ratio at solar system birth was extremely high ($> 1 \times 10^{-2}$). This latter scenario is, however, not consistent with the prediction of the maximum abundance of ^{36}Cl produced either by SEP irradiation ($^{36}\text{Cl}/^{35}\text{Cl} < 1.5 \times 10^{-4}$) or by stellar nucleosynthesis (Wasserburg et al., 2006). For example, assuming coproduction of ^{36}Cl and ^{26}Al in a nearby supernova and simultaneous injection into the solar nebula, initial $^{36}\text{Cl}/^{35}\text{Cl}$ ratios should be $< 2 \times 10^{-4}$ for a canonical ^{26}Al abundance (Wasserburg et al., 1998). This expected ratio is at least one order of magnitude lower than the ^{36}Cl abundance needed to explain the CAI isotope data in the context of assumed concordant decay between ^{26}Al and ^{36}Cl . For these reasons, previous studies have favored a late irradiation of dust and gas to produce ^{36}Cl in the solar nebula. In this framework, ^{36}Cl was then introduced into CAIs through late aqueous alteration after ^{26}Al extinction.

We infer an initial $^{36}\text{Cl}/^{35}\text{Cl}$ model ratio for *Curious Marie* to be $(2.3 \pm 0.6) \times 10^{-5}$ based on the estimated bulk $^{35}\text{Cl}/^{34}\text{S}$ ratio (935 ± 240) and the measured ^{36}S excesses ($^{36}\text{S}/^{34}\text{S}^* = 0.003746 \pm 0.000044$). For comparison, we summarize in Table 2 and Fig. 7 the analyses of ^{26}Al - ^{26}Mg and ^{36}Cl - ^{36}S systematics in secondary phases of CAIs measured in previous work and in this study. The ESS initial $^{36}\text{Cl}/^{35}\text{Cl}$ ratios were calculated using the $^{26}\text{Al}/^{27}\text{Al}$ ratios measured in the surrounding secondary phases through the following equation,

$$\left(\frac{^{36}\text{Cl}}{^{35}\text{Cl}}\right)_{\text{initial}} = \left(\frac{^{36}\text{Cl}}{^{35}\text{Cl}}\right)_{\text{sample}} \left[\frac{(^{26}\text{Al}/^{27}\text{Al})_{\text{initial}}}{(^{26}\text{Al}/^{27}\text{Al})_{\text{sample}}}\right]^{\frac{^{36}\text{Cl}}{^{26}\text{Al}}} \quad (11)$$

As shown in Fig. 7, assuming concordant decay of ^{26}Al and ^{36}Cl , the ESS initial $^{36}\text{Cl}/^{35}\text{Cl}$ ratios derived from previous studies (Lin et al., 2005; Hsu et al., 2006; Ushikubo et al., 2007; Nakashima et al., 2008; Jacobsen et al., 2011) vary widely among CAIs. In addition, all the inferred initial ratios exceed the upper limit for stellar production thus necessitating a significant contribution of ^{36}Cl from SEP irradiation.

We estimated the ESS $^{36}\text{Cl}/^{35}\text{Cl}$ ratio using the calculated $^{36}\text{Cl}/^{35}\text{Cl}$ and $^{26}\text{Al}/^{27}\text{Al}$ model ratios in *Curious Marie*. It is possible that the observed ^{36}Cl - ^{36}S result in *Curious Marie* is derived from late alteration by a Cl-rich fluid, but this process would have most likely compromised the Mg isotopic composition of this CAI, as is the case for many previously studied samples (Hutcheon and Newton, 1981; Lin et al., 2005; Hsu et al., 2006; Fagan et al., 2007; Ushikubo et al., 2007). Therefore, an early aqueous alteration process, which introduced ^{36}Cl into *Curious Marie*, is most consistent with the observed Mg and S isotopic compositions of this sample. If so, ^{36}Cl and ^{26}Al must have coexisted early in the solar nebula, and the $^{36}\text{Cl}/^{35}\text{Cl}$ model ratio $[(2.3 \pm 0.6) \times 10^{-5}$; red rectangle in Fig. 7] would then reflect the $^{36}\text{Cl}/^{35}\text{Cl}$ ratio at the time when the aqueous alteration took place. Given that this event must have been

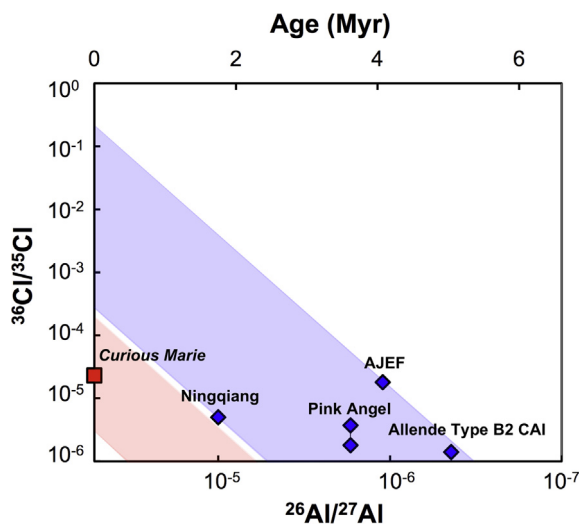


Fig. 7. ^{26}Al - ^{26}Mg and ^{36}Cl - ^{36}S systematics in secondary phases of CAIs obtained in previous work (blue diamonds, data from Lin et al., 2005; Hsu et al., 2006; Ushikubo et al., 2007; Nakashima et al., 2008; Jacobsen et al., 2011) and *Curious Marie* (red rectangle). The inferred $^{36}\text{Cl}/^{35}\text{Cl}$ initial ratios deduced from previous work ranges from 2.9×10^{-4} to 2.2×10^{-1} (blue area), higher than the expected ratio inherited from ISM ($3 \times 10^{-6} \sim 2 \times 10^{-4}$; red area). The $^{36}\text{Cl}/^{35}\text{Cl}$ model ratio in *Curious Marie* is determined as $(2.3 \pm 0.6) \times 10^{-5}$, giving an initial $^{36}\text{Cl}/^{35}\text{Cl}$ ratio of $1.7\text{--}3 \times 10^{-5}$. (For interpretation of the references to color in this figure legend, the reader is referred to the web version of this article.)

occurred no later than the first 50 kyr, we can constrain the initial $^{36}\text{Cl}/^{35}\text{Cl}$ ratio on the *Curious Marie* parent body to be $1.8\text{--}3 \times 10^{-5}$, which falls within the range expected if ^{36}Cl came from a stellar source.

Although ^{36}Cl can also be an irradiation product via reactions between energetic particles and S, Cl, K and Ca, we argue that in the case of *Curious Marie*, irradiation is unlikely to be the main ^{36}Cl contributor. Based on chemistry and petrology, *Curious Marie* almost certainly obtained this radionuclide via interaction with a fluid inside an early-formed icy planetesimal no later than 50,000 years after CAI formation. However, ^{36}Cl could not have been produced in abundance in such a cold nebular region by solar irradiation at that time because intervening dust and gas would have shielded targets from energetic charged particles. For protons with energy of 10 MeV/nucleon, the stopping column density is $\sim 0.2 \text{ g cm}^{-2}$ (Reedy, 1990). Assuming a mass density of $10^{-10}\text{--}10^{-11} \text{ g cm}^{-3}$ (estimated for the midplane at 1 AU for a minimum mass solar nebula; Brauer et al., 2008), the stopping distance for energetic protons is only a fraction of an AU. Another possibility is production of ^{36}Cl in the precursor of *Curious Marie* near the Sun. Even though it is possible to produce $^{36}\text{Cl}/^{35}\text{Cl}$ at the observed level (e.g., Gounelle et al., 2006), the absolute abundances of ^{35}Cl and ^{36}Cl in the irradiated solid would be ≤ 100 ppb (calculations were done by using the cross sections estimated with the TALYS program; Koning and Rochman, 2008). Such low abundances of spallogenic Cl would be completely diluted by a Cl-rich fluid, resulting in a much diminished $^{36}\text{Cl}/^{35}\text{Cl}$ ratio in the secondary minerals. Therefore, we conclude that early Solar System irradiation contributed very little, if at all, to the observed $^{36}\text{Cl}/^{35}\text{Cl}$ ratio in the *Curious Marie* CAI.

The presence of ^{26}Al and ^{36}Cl in *Curious Marie* at the time of aqueous alteration is best explained as inheritance from the molecular cloud, or perhaps from a specific stellar source (Wasserburg et al., 2006; supplementary material from Lugaro et al., 2014; Young, 2014). However, such a source for the ^{36}Cl in *Curious Marie* does not rule out the presence a spallation origin for the ^{36}Cl observed in the secondary minerals from other CAIs and chondrules, as these phases formed much later (~ 3 Myr after CAI) and by that time, any ^{36}Cl of stellar origin would have essentially completely decayed. Further work will be required to determine the proportion of ^{36}Cl coming from inheritance versus that produced by irradiation processes late in the history of the solar nebula.

5. CONCLUSION

We investigated the oxygen isotopic compositions, and the $^{26}\text{Al}\text{--}^{26}\text{Mg}$ and $^{36}\text{Cl}\text{--}^{36}\text{S}$ systems in the U-depleted CAI, *Curious Marie*. Based on this study, we conclude that

- (1) Homogenous and elevated ^{26}Mg and ^{36}S excesses were observed in the secondary phases of the Allende CAI *Curious Marie*, indicating an intense alteration by a Na, Cl-rich oxidizing fluid. The alteration resulted in formation of new minerals, primarily nepheline and sodalite, and also in significant deple-

tion of uranium and magnesium from the bulk CAI. The fluid brought in live ^{36}Cl which was incorporated into the new minerals along with the existing ^{26}Al that was still close to its canonical solar system initial value.

- (2) Thermal modeling suggests that the aqueous alteration of *Curious Marie* most likely occurred in the outer regions of an early-accreted small icy planetesimal. After a few million years, during which time ^{26}Al and ^{36}Cl decayed to their radiogenic daughters, this small icy body was broken up and fragments incorporated into the parent body of CV chondrites. In the CV parent body, thermal processing caused by impacts or continuous accretion gave rise to closed-system isotopic equilibration in *Curious Marie* to homogenize ^{26}Mg and ^{36}S excesses without contamination with chondritic components.
- (3) The isotopic system and petrology in *Curious Marie* CAI suggest the presence of pre-accretionary small icy bodies in the early solar system prior to the formation of Allende parent body. Those early formed planetesimals were disrupted and their debris was recycled into a second generation of planetesimals.
- (4) The ^{26}Mg and ^{36}S excesses present in the early-altered *Curious Marie* provide evidence that ^{26}Al and ^{36}Cl co-existed in the early solar nebula. The $^{36}\text{Cl}/^{35}\text{Cl}$ ratio at the time of early alteration can be constrained as $(2.3 \pm 0.6) \times 10^{-5}$. Since alteration took place when ^{26}Al was still near the canonical abundance, we inferred that the initial $^{36}\text{Cl}/^{35}\text{Cl}$ in ESS should be $1.7\text{--}3 \times 10^{-5}$.
- (5) The early alteration event that leached U from *Curious Marie* was also responsible for the Mg depletion, allowing us to use $^{26}\text{Al}\text{--}^{26}\text{Mg}$ to constrain the time of Cm/U fractionation in this CAI. Given that the alteration occurred very early, the inferred $^{247}\text{Cm}/^{235}\text{U}$ ratio of $(5.6 \pm 0.3) \times 10^{-5}$ in *Curious Marie* should also represent the Solar System initial ^{247}Cm abundance.

ACKNOWLEDGEMENT

We thank Yuri Amelin, Yunbin Guan, and Benjamin Jacobsen for comments on the manuscript. We are particularly grateful to Edward D. Young and Katelyn A. McCain for their help with simulations of the thermal evolution for the small planetesimals. We also thank Heng Yang for his assistance on contour maps. The *Curious Marie* sample from the Allende meteorite was provided by the Robert A. Pritzker Center for Meteoritics (Field Museum). Discussions with Alexander N. Krot, Benjamin Jacobsen, Edward D. Young, and Craig E. Manning are greatly appreciated. This work was supported by NASA Grant (NNX13AD13G) to K.D. M., and a Crosby Postdoctoral Fellowship to F.L.H.T. The UCLA ion microprobe facility is partially supported by a grant from the NSF Instrumentation and Facilities program.

APPENDIX A. SUPPLEMENTARY MATERIAL

Supplementary data associated with this article can be found, in the online version, at <http://dx.doi.org/10.1016/j.gca.2017.03.001>.

REFERENCES

- Aléon J., Krot A. N., McKeegan K. D., MacPherson G. J. and Ulyanov A. A. (2005) Fine-grained, spinel-rich inclusions from the reduced CV chondrite Efremovka: II. Oxygen isotopic compositions. *Meteor. Planet. Sci.* **40**, 1043–1058.
- Anderson D. H. and Hawkes H. E. (1958) Relative mobility of the common elements in weathering of some schist and granite areas. *Geochim. Cosmochim. Acta* **14**, 204–210.
- Arnould M., Goriely S. and Meynet G. (2006) The production of short-lived radionuclides by new non-rotating and rotating Wolf-Rayet model stars. *Astron. Astrophys.* **453**, 653–659.
- Arnould M., Paulus G. and Meynet G. (1997) Short-lived radionuclide production by non-exploding Wolf-Rayet stars. *Astron. Astrophys.* **321**, 452–464.
- Baker J., Bizzarro M., Wittig N., Connelly J. and Haack H. (2005) Early planetesimal melting from an age of 4.5662 Gyr for differentiated meteorites. *Nature* **436**, 1127–1131.
- Barrer R. M. and White E. A. D. (1952) The hydrothermal chemistry of silicates. Part II. Synthetic crystalline sodium aluminosilicates. *J. Chem. Soc. (Resumed)*, 1561–1571.
- Bischoff A. (1998) Aqueous alteration of carbonaceous chondrites: evidence for preaccretionary alteration—a review. *Meteor. Planet. Sci.* **33**, 1113–1122.
- Boynton W. V. (1975) Fractionation in the solar nebula: condensation of yttrium and the rare earth elements. *Geochim. Cosmochim. Acta* **39**, 569–584.
- Brauer F., Dullemond C. P. and Henning T. (2008) Coagulation, fragmentation and radial motion of solid particles in protoplanetary disks. *Astron. Astrophys.* **480**, 859–877.
- Brearley A. J. and Krot A. N. (2013) Metasomatism in the early solar system: The record from chondritic meteorites. *Metasomat. Chem. Transform. Rock*, 659–789.
- Brennecka G. A., Weyer S., Wadhwa M., Janney P. E., Zipfel J. and Anbar A. D. (2010) $^{238}\text{U}/^{235}\text{U}$ variations in meteorites: extant ^{247}Cm and implications for Pb-Pb dating. *Science* **327**, 449–451.
- Bricker G. E. and Caffee M. W. (2013) Incorporation of ^{36}Cl into Calcium-Aluminum-Rich Inclusions in the Solar Wind Implantation Model. *Adv. Astron.*, 2013.
- Buchanan P. C., Zolensky M. E. and Reid A. M. (1997) Petrology of Allende dark inclusions. *Geochim. Cosmochim. Acta* **61**, 1733–1743.
- Catanzaro E. J., Murphy T. J., Garner E. L. and Shields W. R. (1966) Absolute isotopic abundance ratios and atomic weight of magnesium. *J. Res. Nat. Bur. Stand.* **A70**, 453–458.
- Chaussidon M. and Gounelle M. (2006) Irradiation processes in the early solar system. *Meteor. Early Solar System II* **1**, 323–339.
- Clayton D. D. (1985) Galactic chemical evolution and nucleocosmochronology-analytic quadratic models. *Astrophys. J.* **288**, 569–574.
- Clayton D. D. (1988) Nuclear cosmochronology within analytic models of the chemical evolution of the solar neighbourhood. *Mont. Not. R. Astron. Soc.* **234**, 1–36.
- Clayton R. N. and Mayeda T. K. (1984) The oxygen isotope record in Murchison and other carbonaceous chondrites. *Earth Planet. Sci. Lett.* **67**, 151–161.
- Cohen R. E., Kornacki A. S. and Wood J. A. (1983) Mineralogy and petrology of chondrules and inclusions in the Mokoia CV3 chondrite. *Geochim. Cosmochim. Acta* **47**, 1739–1757.
- Dauphas N. and Chaussidon M. (2011) A perspective from extinct radionuclides on a young stellar object: the sun and its accretion disk. *Ann. Rev. Earth Planet. Sci.* **39**, 351–386.
- Davis A. M. and Grossman L. (1979) Condensation and fractionation of rare earths in the solar nebula. *Geochim. Cosmochim. Acta* **43**, 1611–1632.
- Davis A. M., Richter F. M., Mendybaev R. A., Janney P. E., Wadhwa M. and McKeegan K. D. (2015) Isotopic mass fractionation laws for magnesium and their effects on ^{26}Al - ^{26}Mg systematics in solar system materials. *Geochim. Cosmochim. Acta* **158**, 245–261.
- Ding T., Valkiers S., Kipphardt H., De Bievre P., Taylor P. D. P., Gonfiantini R. and Krouse R. (2001) Calibrated sulfur isotope abundance ratios of three IAEA sulfur isotope reference materials and V-CDT with a reassessment of the atomic weight of sulfur. *Geochim. Cosmochim. Acta* **65**, 2433–2437.
- Duprat J. and Tatischeff V. (2007) Energetic constraints on in situ production of short-lived radionuclides in the early solar system. *Astrophys. J. Lett.* **671**, L69–L72.
- Elkins-Tanton L. T., Weiss B. P. and Zuber M. T. (2011) Chondrites as samples of differentiated planetesimals. *Earth Planet. Sci. Lett.* **305**, 1–10.
- Fagan T. J., Guan Y. and MacPherson G. J. (2007) Al-Mg isotopic evidence for episodic alteration of Ca-Al-rich inclusions from Allende. *Meteor. Planet. Sci.* **42**, 1221–1240.
- Fruchter J. S. (1998) *Uranium Mobility During In Situ Redox Manipulation of the 100 Areas of the Hanford Site*. Pacific Northwest National Laboratory, Richland, WA.
- Gaidos E., Krot A. N., Williams J. P. and Raymond S. N. (2009) ^{26}Al and the formation of the solar system from a molecular cloud contaminated by Wolf-Rayet winds. *Astrophys. J.* **696**, 1854–1863.
- Galy A., Young E. D., Ash R. D. and O’Nions R. K. (2000) The formation of chondrules at high gas pressures in the solar nebula. *Science* **290**, 1751–1753.
- Goswami J. N., Marhas K. K., Chaussidon M., Gounelle M. and Meyer B. S. (2005) Origin of short-lived radionuclides in the early solar system. *Chond. Protoplanet. Disk ASP Conf. Ser.* **341**(December), 485–514.
- Gounelle M. and Meynet G. (2012) Solar system genealogy revealed by extinct short-lived radionuclides in meteorites. *Astron. Astrophys.* **545**, A4–A13.
- Gounelle M. (2015) The abundance of ^{26}Al -rich planetary systems in the Galaxy. *Astron. Astrophys.* **582**, A26–A33.
- Gounelle M., Shu F. H., Shang H., Glassgold A. E., Rehm K. E. and Lee T. (2006) The irradiation origin of beryllium radioisotopes and other short-lived radionuclides. *Astrophys. J.* **640**, 1163–1170.
- Hashimoto A. and Grossman L. (1987) Alteration of Al-rich inclusions inside amoeboid olivine aggregates in the Allende meteorite. *Geochim. Cosmochim. Acta* **51**, 1685–1704.
- Herndon J. M. and Herndon M. A. (1977) Aluminum-26 as a planetoid heat source in the early Solar System. *Meteoritics* **12**, 459–465.
- Hsu W., Guan Y., Leshin L. A., Ushikubo T. and Wasserburg G. J. (2006) A late episode of irradiation in the early solar system: evidence from extinct ^{36}Cl and ^{26}Al in meteorites. *Astrophys. J.* **640**, 525–529.
- Huss G. R., Meyer B. S., Srinivasan G., Goswami J. N. and Sahijpal S. (2009) Stellar sources of the short-lived radionuclides in the early solar system. *Geochim. Cosmochim. Acta* **73**, 4922–4945.
- Hutcheon I. D. and Hutchison R. (1989) Evidence from the Semarkona ordinary chondrite for ^{26}Al heating of small planets. *Nature* **337**, 238–241.
- Hutcheon, I.D., Newton, R.C., 1981, March. Mg isotopes, mineralogy and mode of formation of secondary phases in C3 refractory inclusions. In: Lunar and Planetary Science Conference XII, pp. 491–493.

- Isa, J., Kohl, I.E., Wasson, J.T., Young, E.D. and McKeegan, K. D., 2016. Quantification of Oxygen Isotope SIMS Matrix Effects in Olivine Samples: Correlation with Sputter Rate. Lunar and Planetary Science Conference XLVII, #3004.
- Jacobsen B., Matzel J., Hutcheon I. D., Krot A. N., Yin Q. Z., Nagashima K., Ramon E. C., Weber P. K., Ishii H. A. and Ciesla F. J. (2011) Formation of the short-lived radionuclide ^{36}Cl in the protoplanetary disk during late-stage irradiation of a volatile-rich reservoir. *Astrophys. J. Lett.* **731**, L28–L34.
- Jacobsen B., Yin Q. Z., Moynier F., Amelin Y., Krot A. N., Nagashima K., Hutcheon I. D. and Palme H. (2008) ^{26}Al - ^{26}Mg and ^{207}Pb - ^{206}Pb systematics of Allende CAIs: canonical solar initial $^{26}\text{Al}/^{27}\text{Al}$ ratio reinstated. *Earth Planet. Sci. Lett.* **272**, 353–364.
- Jochum K. P., Weis U., Stoll B., Kuzmin D., Yang Q., Raczek I., Jacob D. E., Stracke A., Birbaum K., Frick D. A. and Günther D. (2011) Determination of reference values for NIST SRM 610–617 glasses following ISO guidelines. *Geostand. Geoanal. Res.* **35**, 397–429.
- Jogo K., Nakamura T., Noguchi T. and Zolotov M. Y. (2009) Fayalite in the Vigarano CV3 carbonaceous chondrite: occurrences, formation age and conditions. *Earth Planet. Sci. Lett.* **287**, 320–328.
- Jura M., Xu S. and Young E. D. (2013) ^{26}Al in the early Solar System: Not so unusual after all. *Astrophys. J. Lett.* **775**, L41–L45.
- Kasemann S., Meixner A., Rocholl A., Vennemann T., Rosner M., Schmitt A. K. and Wiedenbeck M. (2001) Boron and oxygen isotope composition of certified reference materials NIST SRM 610/612 and reference materials JB-2 and JR-2. *Geostand. Newslett.* **25**, 405–416.
- Keller L. P. and Buseck P. R. (1989) Aqueous alteration of the Kaba CV3 carbonaceous chondrite. *Meteoritics* **24**, 284.
- Kimura M. and Ikeda Y. (1995) Anhydrous alteration of Allende chondrules in the solar nebula II: alkali-Ca exchange reactions and formation of nepheline, sodalite and Ca-rich phases in chondrules. *Antarctic Meteor. Res.* **8**, 123–138.
- Kita N. T., Nagahara H., Tachibana S., Tomomura S., Spicuzza M. J., Fournelle J. H. and Valley J. W. (2010) High precision SIMS oxygen three isotope study of chondrules in LL3 chondrites: role of ambient gas during chondrule formation. *Geochim. Cosmochim. Acta* **74**, 6610–6635.
- Kojima T. and Tomeoka K. (1996) Indicators of aqueous alteration and thermal metamorphism on the CV parent body: microtextures of a dark inclusion from Allende. *Geochim. Cosmochim. Acta* **60**, 2651–2666.
- Koning A. J. and Rochman D. (2008) Towards sustainable nuclear energy: putting nuclear physics to work. *Ann. Nucl. Energy* **35**, 2024–2030.
- Krot, A.N., Nagashima, K., Hutcheon, I.D., Ishii, H.A., Jacobsen, B., Yin, Q.Z., Davis, A.M., Simon, S.B., 2010. Mineralogy, petrography, oxygen and magnesium isotopic compositions and formation age of grossular-bearing assemblages in the Allende CAIs. In: Lunar and Planetary Science Conference XLI, March, p. 1406.
- Krot A. N., Petaev M. I. and Bland P. A. (2004) Multiple formation mechanisms of ferrous olivine in CV carbonaceous chondrites during fluid-assisted metamorphism. *Antarctic Meteor. Res.* **17**, 153–171.
- Krot A. N., Scott E. R. and Zolensky M. E. (1997) Origin of fayalitic olivine rims and lath-shaped matrix olivine in the CV3 chondrite Allende and its dark inclusions. *Meteor. Planet. Sci.* **32**, 31–49.
- Langmuir D. (1978) Uranium solution-mineral equilibria at low temperatures with applications to sedimentary ore deposits. *Geochim. Cosmochim. Acta* **42**, 547–569.
- Larsen K. K., Trinquier A., Paton C., Schiller M., Wielandt D., Ivanova M. A., Connelly J. N., Nordlund Å., Krot A. N. and Bizzarro M. (2011) Evidence for magnesium isotope heterogeneity in the solar protoplanetary disk. *Astrophys. J. Lett.* **735**, L37–L44.
- LaTourrette T. and Wasserburg G. J. (1998) Mg diffusion in anorthite: implications for the formation of early solar system planetesimals. *Earth Planet. Sci. Lett.* **158**, 91–108.
- Leya I., Halliday A. N. and Wieler R. (2003) The predictable collateral consequences of nucleosynthesis by spallation reactions in the early solar system. *Astrophys. J.* **594**, 605–616.
- Lin Y., Guan Y., Leshin L. A., Ouyang Z. and Wang D. (2005) Short-lived chlorine-36 in a Ca- and Al-rich inclusion from the Ningqiang carbonaceous chondrite. *Proceedings of the National Academy of Sciences of the United States of America* **102**, 1306–1311.
- Liu M. C., Chaussidon M., Srinivasan G. and McKeegan K. D. (2012) A lower initial abundance of short-lived ^{41}Ca in the early solar system and its implications for solar system formation. *Astrophys. J.* **761**, 137–144.
- Luce R. W., Bartlett R. W. and Parks G. A. (1972) Dissolution kinetics of magnesium silicates. *Geochim. Cosmochim. Acta* **36**, 35–50.
- Ludwig K.R., 2012. Isoplot 3.75: A geochronological toolkit for Microsoft Excel. Berkeley Geochronology Center Special Publication No. 5.
- Lugaro M., Heger A., Osrin D., Goriely S., Zuber K., Karakas A. I., Gibson B. K., Doherty C. L., Lattanzio J. C. and Ott U. (2014) Stellar origin of the ^{182}Hf cosmochronometer and the presolar history of solar system matter. *Science* **345**, 650–653.
- MacPherson G. J., Bullock E. S., Janney P. E., Kita N. T., Ushikubo T., Davis A. M., Wadhwa M. and Krot A. N. (2010) Early solar nebula condensates with canonical, not supra-canonical, initial $^{26}\text{Al}/^{27}\text{Al}$ ratios. *Astrophys. J. Lett.* **711**, L117–L121.
- Marhas K. K., Goswami J. N. and Davis A. M. (2002) A limit on the energetic particle irradiation of the solar nebula. *Meteor. Planet. Sci. Suppl.* **37**, 94.
- Markowski, A., Quitté, G., Kleine, T., Bizzarro, M., Leya, I., Wieler, R., Ammon, K., Halliday, A.N., 2006. Early and rapid differentiation of planetesimals inferred from isotope data in iron meteorites and angrites. In: Lunar and Planetary Science Conference XXXVII, March, p. 2000.
- Matson, D.L., Castillo-Rogez, J.C., Johnson, T.V., Turner, N., Lee, M.H., Lunine, J.I., 2009. ^{26}Al decay: heat production and revised age for iapetus. In: Lunar and Planetary Science Conference XL, p. 2191.
- McKeegan K.D., Davis A.M., 2004. Early solar system chronology. In: Davis A.M. (Ed.), Meteorites, Comets, and Planets, 1.16. Elsevier Pergamon, pp. 431–475.
- McKeegan K. D., Chaussidon M. and Robert F. (2000) Incorporation of short-lived ^{10}Be in a calcium-aluminum-rich inclusion from the Allende meteorite. *Science* **289**, 1334–1337.
- McKeegan K. D., Leshin L. A., Russell S. S. and MacPherson G. J. (1998) Oxygen isotopic abundances in calcium-aluminum-rich inclusions from ordinary chondrites: implications for nebular heterogeneity. *Science* **280**, 414–418.
- Mendybaev R. A., Richter F. M., Georg R. B., Janney P. E., Spicuzza M. J., Davis A. M. and Valley J. W. (2013) Experimental evaporation of Mg- and Si-rich melts: implications for the origin and evolution of FUN CAIs. *Geochim. Cosmochim. Acta* **123**, 368–384.
- Metzler K., Bischoff A. and Stöfler D. (1992) Accretionary dust mantles in CM chondrites: evidence for solar nebula processes. *Geochim. Cosmochim. Acta* **56**, 2873–2897.

- Meyer B. S. and Clayton D. (2000) Short-lived radioactivities and the birth of the Sun. *Space Sci. Rev.* **92**, 133–152.
- Murty S. V. S., Goswami J. N. and Shukolyukov Y. A. (1997) Excess ^{36}Ar in the Efremovka meteorite: a strong hint for the presence of ^{36}Cl in the early solar system. *Astrophys. J. Lett.* **475**, L65–L68.
- Nakashima D., Ott U., Hoppe P. and El Goresy A. (2008) Search for extinct ^{36}Cl : Vigarano CAIs, the Pink Angel from Allende, and a Ningqiang chondrule. *Geochim. Cosmochim. Acta* **72**, 6141–6153.
- Nittler L.R., Dauphas N., 2006. Meteorites and the chemical evolution of the Milky Way. In: Lauretta, D.S., McSween Jr., H.Y. (Eds.), *Meteorites and the Early Solar System II*, vol. 943. University of Arizona Press, Tucson, pp. 127–146.
- Nyquist L. E., Reese Y., Wiesmann H., Shih C.-Y. and Takeda H. (2001) Live ^{53}Mn and ^{26}Al in a unique cumulate eucrite with very calcic feldspar (An~98). *Meteor. Planet. Sci.* **36**, A151.
- Nyquist L. E., Reese Y., Wiesmann H., Shih C.-Y. and Takeda H. (2003b) Fossil ^{26}Al and ^{53}Mn in the Asuka-881394 eucrite: evidence of the earliest crust on planetesimal 4 Vesta. *Earth Planet. Sci. Lett.* **214**, 11–25.
- Nyquist L. E., Shih C.-Y., Wiesmann H., Yamaguchi A. and Misawa K. (2003a) Early volcanism on the NWA 011 parent body. *Meteor. Planet. Sci.* **38**, A59.
- Ogliore R. C., Huss G. R. and Nagashima K. (2011) Ratio estimation in SIMS analysis. *Nucl. Instrum. Meth. Phys. Res. Sect. B: Beam Interact. Mater. Atoms* **269**, 1910–1918.
- Reedy, R.C., 1990. Cosmogenic-radionuclide production rates in mini-spherules. In: *Lunar and Planetary Science Conference XXI*, p. 1001.
- Rowe M. W., Clayton R. N. and Mayeda T. K. (1994) Oxygen isotopes in separated components of CI and CM meteorites. *Geochim. Cosmochim. Acta* **58**, 5341–5347.
- Russell, S.S., MacPherson, G.J., 1997. Alteration of calcium-aluminium-rich inclusions: times and places. In: *Parent-Body and Nebular Modification of Chondritic Materials*, vol. 1, p. 54.
- Sahijpal S. and Gupta G. (2011) Did the carbonaceous chondrites evolve in the crustal regions of partially differentiated asteroids? *J. Geophys. Res.: Planets* **116**, E6.
- Sahijpal S., Soni P. and Gupta G. (2007) Numerical simulations of the differentiation of accreting planetesimals with ^{26}Al and ^{60}Fe as the heat sources. *Meteor. Planet. Sci.* **42**, 1529–1548.
- Schiller M., Baker J. A. and Bizzarro M. (2010) ^{26}Al - ^{26}Mg dating of asteroidal magmatism in the young Solar System. *Geochim. Cosmochim. Acta* **74**, 4844–4864.
- Schott J., Berner R. A. and Sjöberg E. L. (1981) Mechanism of pyroxene and amphibole weathering—I. Experimental studies of iron-free minerals. *Geochim. Cosmochim. Acta* **45**, 2123–2135.
- Sharp Z. D., Helffrich G. R., Bohlen S. R. and Essene E. J. (1989) The stability of sodalite in the system $\text{NaAlSi}_3\text{O}_8$ - NaCl . *Geochim. Cosmochim. Acta* **53**, 943–1954.
- Siever R. and Woodford N. (1979) Dissolution kinetics and the weathering of mafic minerals. *Geochim. Cosmochim. Acta* **43**, 717–724.
- Slodzian G., Hillion F., Stadermann F. J. and Zinner E. (2004) QSA influences on isotopic ratio measurements. *Appl. Surf. Sci.* **231**, 874–877.
- Snow J. E. and Dick H. J. (1995) Pervasive magnesium loss by marine weathering of peridotite. *Geochim. Cosmochim. Acta* **59**, 4219–4235.
- Spivak-Birndorf L., Wadhwa M. and Janney P. (2009) ^{26}Al - ^{26}Mg systematics in D'Orbigny and Sahara 99555 angrites: implications for high-resolution chronology using extinct chronometers. *Geochim. Cosmochim. Acta* **73**, 5202–5211.
- Šrámek O., Milelli L., Ricard Y. and Labrosse S. (2012) Thermal evolution and differentiation of planetesimals and planetary embryos. *Icarus* **217**, 339–354.
- Srinivasan G. (2002) ^{26}Al - ^{26}Mg systematics in eucrites A881394, A87122 and Vissannapeta. *Meteor. Planet. Sci. Suppl.* **37**, 135.
- Srinivasan G., Goswami J. N. and Bhandari N. (1999) ^{26}Al in eucrite Piplia Kalan: plausible heat source and formation chronology. *Science* **284**, 1348–1350.
- Sugiura N., Miyazaki A. and Yanai K. (2005) Widespread magmatic activities on the angrite parent body at 4562 Ma ago. *Earth, Planets Space* **57**, E13–E16.
- Tang H. and Dauphas N. (2012) Abundance, distribution, and origin of ^{60}Fe in the solar protoplanetary disk. *Earth Planet. Sci. Lett.* **359–360**, 248–263.
- Tatischeff V., Duprat J. and De Sereville N. (2010) A runaway Wolf-Rayet star as the origin of ^{26}Al in the early Solar System. *Astrophys. J. Lett.* **714**, L26–L30.
- Thrane K., Bizzarro M. and Baker J. A. (2006) Extremely brief formation interval for refractory inclusions and uniform distribution of ^{26}Al in the early solar system. *Astrophys. J. Lett.* **646**, L159–L162.
- Tissot F. L. H., Dauphas N. and Grossman L. (2016) Origin of uranium isotope variations in early solar nebula condensates. *Sci. Adv.* **2**, e1501400.
- Trappitsch R. and Ciesla F. J. (2015) Solar cosmic-ray interaction with protoplanetary disks: production of short-lived radionuclides and amorphization of crystalline material. *Astrophys. J.* **805**, 5–16.
- Trinquier A., Birck J. L., Allegre C. J., Göpel C. and Ulfbeck D. (2008) ^{53}Mn - ^{53}Cr systematics of the early Solar System revisited. *Geochim. Cosmochim. Acta* **72**, 5146–5163.
- Turner G., Crowther S. A., Burgess R., Gilmour J. D., Kelley S. P. and Wasserburg G. J. (2013) Short lived ^{36}Cl and its decay products ^{36}Ar and ^{36}S in the early solar system. *Geochim. Cosmochim. Acta* **123**, 358–367.
- Ushikubo T., Guan Y., Hiyagon H., Sugiura N. and Leshin L. A. (2007) ^{36}Cl , ^{26}Al , and O isotopes in an Allende type B2 CAI: implications for multiple secondary alteration events in the early solar system. *Meteor. Planet. Sci.* **42**, 1267–1279.
- Veit T., Buhl J. C. and Hoffmann W. (1991) Hydrothermal synthesis, characterization and structure refinement of chlorate- and perchlorate-sodalite. *Catal. Today* **8**, 405–413.
- Villeneuve J., Chaussidon M. and Libourel G. (2009) Homogeneous distribution of ^{26}Al in the solar system from the Mg isotopic composition of chondrules. *Science* **325**, 985–988.
- Wadhwa M., Srinivasan G. and Carlson R. W. (2006) Timescales of planetesimal differentiation in the early solar system. *Meteor. Early Solar System II*, 715–731.
- Wanner, H. and Forest, I. (eds.) (1992) *Chemical Thermodynamics of Uranium*, vol. 1. North-Holland, Amsterdam.
- Wasserburg G. J., Gallino R. and Busso M. (1998) A test of the supernova trigger hypothesis with ^{60}Fe and ^{26}Al . *Astrophys. J. Lett.* **500**, L189–L193.
- Wasserburg G. J., Busso M., Gallino R. and Nollett K. M. (2006) Short-lived nuclei in the early Solar System: possible AGB sources. *Nucl. Phys. A* **777**, 5–69.
- Wasserburg G. J., Hutcheon I. D., Aléon J., Ramon E. C., Krot A. N., Nagashima K. and Brearley A. J. (2011) Extremely Na- and Cl-rich chondrule from the CV3 carbonaceous chondrite Allende. *Geochim. Cosmochim. Acta* **75**, 4752–4770.
- Wilson L., Keil K. and Love S. G. (1998) Factors controlling the bulk densities of asteroids. *Meteor. Planet. Sci. Suppl.* **33**, 168.
- Wilson L., Keil K. and Love S. J. (1999) The internal structures and densities of asteroids. *Meteor. Planet. Sci.* **34**, 479–483.

- Young E. D. (2001) The hydrology of carbonaceous chondrite parent bodies and the evolution of planet progenitors. *Philos. Trans. R. Soc. Lond. A: Math., Phys. Eng. Sci.* **359**, 2095–2110.
- Young E. D. (2014) Inheritance of solar short-and long-lived radionuclides from molecular clouds and the unexceptional nature of the solar system. *Earth Planet. Sci. Lett.* **392**, 16–27.
- Zhou Q., Yin Q. Z., Young E. D., Li X. H., Wu F. Y., Li Q. L., Liu Y. and Tang G. Q. (2013) SIMS Pb–Pb and U–Pb age determination of eucrite zircons at $<5 \mu\text{m}$ scale and the first 50 Ma of the thermal history of Vesta. *Geochim. Cosmochim. Acta* **110**, 152–175.

Associate editor: Yuri Amelin